



Challenges and Applications of Flexible Sodium Ion Batteries

Xiang-Xi He¹, Jia-Hua Zhao¹, Wei-Hong Lai³, Zhuo Yang¹, Yun Gao¹, Hang Zhang³, Yun Qiao¹, Li Li^{1*} , and Shu-Lei Chou^{1,2*} 

¹ School of Environmental and Chemical Engineering, Shanghai University, 99 Shangda Road, Shanghai 200444, China

² Institute for Carbon Neutralization, College of Chemistry and Materials Engineering, Wenzhou University, Wenzhou, Zhejiang 325035, China

³ Institute for Superconducting and Electronic Materials, University of Wollongong, Wollongong, New South Wales 2522, Australia

* Corresponding author, E-mail: LILI2020@shu.edu.cn; chou@wzu.edu.cn

Abstract

Sodium-ion batteries are considered to be a future alternative to lithium-ion batteries because of their low cost and abundant resources. In recent years, the research of sodium-ion batteries in flexible energy storage systems has attracted widespread attention. However, most of the current research on flexible sodium ion batteries is mainly focused on the preparation of flexible electrode materials. In this paper, the challenges faced in the preparation of flexible electrode materials for sodium ion batteries and the evaluation of device flexibility is summarized. Several important parameters including cycle-calendar life, energy/power density, safety, flexible, biocompatibility and multifunctional intergration of current flexible sodium ion batteries will be described mainly from the application point of view. Finally, the promising current applications of flexible sodium ion batteries are summarized.

Key words: Flexible sodium-ion batteries; Solid-State batteries; Dual-Ion Battery; Stretchable; Self-healing; Self-charging; Textile.

Citation: Xiang-Xi He, Jia-Hua Zhao, Wei-Hong Lai, Zhuo Yang, Yun Gao, et al. Challenges and Applications of Flexible Sodium Ion Batteries. *Materials Lab* 2022, 1, 210001. DOI: [10.54227/mlab.20210001](https://doi.org/10.54227/mlab.20210001)

1 Introduction

With the continuous penetration of flexible electronic devices in our lives, the desire and reliance on bendable, implantable and wearable electronic products will become even strong in the future^[1,2]. Flexible lithium-ion batteries and flexible sodium-ion batteries with high energy density will be highly anticipated^[3]. Among them, lithium-ion batteries were first commercialized by Sony in 1991, and it has been nearly 30 years since then, and their technology is becoming increasingly mature. This will lead to exponential growth in the demand for lithium-ion batteries in the fields of electric vehicles, large-scale energy storage, and portable electronic devices. However, lithium reserves are scarce and the cost of lithium sources has been increased dramatically for the past decades^[4]. Sodium ion batteries due to their similar performance and lower cost compared with that lithium ion batteries, can be considered to compete with or replace lithium-ion batteries in the future flexible energy storage devices^[5–7]. In this review, we provide a comprehensive summary of recent advances in flexible sodium-ion battery energy storage devices (Figure 1).

We searched the Web of Science for articles on flexible lithium/sodium ion batteries published in the past 10 years on the topics of "flexible batteries," "flexible lithium ion batteries," "flexible sodium ion batteries." As can be seen from Figure 2, the articles on flexible sodium ion batteries showed a significant growing trend in the early years, but showed a saturated trend in the last two years. It may be that various common

types of potentially flexible electrode materials have basically been explored. It was reported that the common electrodes in flexible sodium ion batteries, mainly consist of graphene^[8], commercial carbon cloth^[9], CNF^[10], CNT^[11], metal substrates^[12] and their composites with inorganics and polymers^[7,13]. These articles often present only the flexible anode or cathode in a half cell. The development of flexible sodium ion batteries requires not only the development of inherently flexible materials but also the consideration of component matching for the full cell and improvements in structural design. Zhi et al.^[14] summarizes future development strategies for flexible lithium-ion batteries and supercapacitors, in terms of mechanical reliability assessment of flexible devices and performance analysis in lithium-ion batteries. Authors provided a detailed analysis of bending mechanics, which not only provided a reliable test method for describing the bending state, but also provided guidance for the design of device structures in the event of mechanical failure. However, these assessments have not attracted much attention on flexible sodium ion batteries. This is because, although some articles have also produced flexible sodium ion full cells, the flexibility has not been tested and evaluated. In addition, the electrochemical performance of these materials may not be that promising, such as, low Initial coulombic efficiency, poor rate performance, low specific capacity and short cycling or calendar life, as well as high manufacturing cost and environmental pollution may occur. Therefore, research on flexible sodium ion batteries must be pursued a balance of

Received 13 October 2021; Accepted 20 January 2022; Published online

© 2022 The Author(s). *Materials Lab* published by Lab Academic Press

various performance indicators or a breakthrough in a particular area to meet the requirements of flexible rechargeable batteries.

This review will first focus on the current challenges facing flexible sodium ion batteries, including the cost of material preparation and the difficulties faced in mass production; how to quantitatively evaluate mechanical deformation tests of devices in flexible sodium ion batteries; the mechanisms by which the electrochemical performance of flexible sodium ion batteries fails due to mechanical deformation; and how to rationally design a full cell. So, we will enumerate several new functional flexible sodium ion full cells and their future prospects in terms of reasonable matching of cathode, anode, electrolyte and encapsulation materials, balance of material preparation methods and optimization of structural design. For example, in terms of material and electrolyte matching, we will present flexible sodium-ion batteries for conventional organic, symmetric, all-solid-state, and dual-ion batteries. From the perspective of functional applications, we will present flexible sodium ion batteries/capacitors, such as stretchable, transparent, self-healing and self-charging types (Figure 1).

2 Challenges for flexible sodium ion batteries

The application range and lifetime of flexible sodium-based energy storage devices depend heavily on their mechanical deformation tolerance and the maintenance of electrochemical properties under deformation. In addition the basic electrochemical properties of the flexible electrode materials themselves are particularly important, such as specific capacity, initial coulomb efficiency, cycling performance, and calendar life also need to meet certain prerequisites for commercialization^[5]. In terms of strain, flexible sodium-ion batteries can also be classified into external mechanical deformation

forms such as bending, compression, stretching, folding, and twisting. In different application scenarios, the direction of deformation and the force required vary somewhat. In addition to electrochemical performance, safety, comfort, convenience and durability will be other key considerations^[15].

2.1 Challenges of flexible electrode preparation

As energy storage devices are made up of various components such as cathode and anode, separator, electrolyte and outer packaging, it is challenging to achieve stable performance for electrochemical energy storage devices under external mechanical stress such as bending and deformation. This means that the components of these batteries need to be flexible so that the full battery assembled from the various flexible cathode and anode and diaphragm packages can operate as stably as possible under external mechanical stress.

An introduction to flexible electrode materials for flexible sodium ion batteries has been presented in a relevant reviews^[6,16]. The main categories of electrode materials are metallic substrates, carbon substrates and other polymeric organic materials^[17]. There are two main types of flexible electrode materials from the perspective of their design. One type is the *in-situ* synthesis of the active material directly on the flexible collector^[12], in which an existing flexible film is used to act as a substrate and the desired active material is then grown simultaneously on the substrate by various strategies (e.g. chemical etching, PVD/impregnation, hydrothermal and solvothermal sol-gel methods, co-precipitation)^[18–23]. Such flexible substrates are generally inactive and do not contribute to specific capacity, but offer some improvement in performance at multiples due to enhanced ions transport and electric conductivity. The other category is electrodes with flexible free-standing films made directly from the active material^[24]. For example, some inherently flexible additives including polymeric organics, carbon nanotubes, graphene,

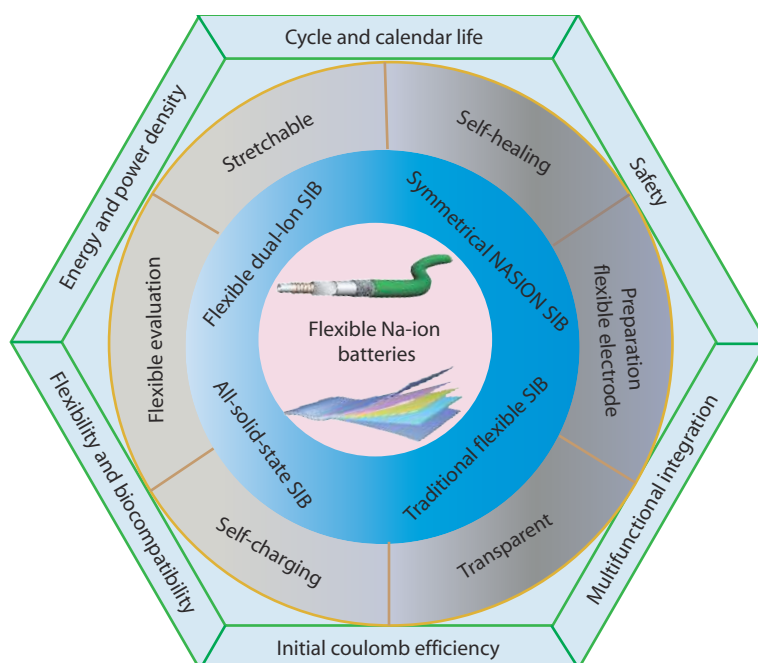


Fig. 1 Challenges and application of flexible sodium ion batteries. Illustrations reproduced with permission. Copyright 2017, Wiley-VCH. Illustrations reproduced with permission^[110] Copyright 2017, Elsevier.

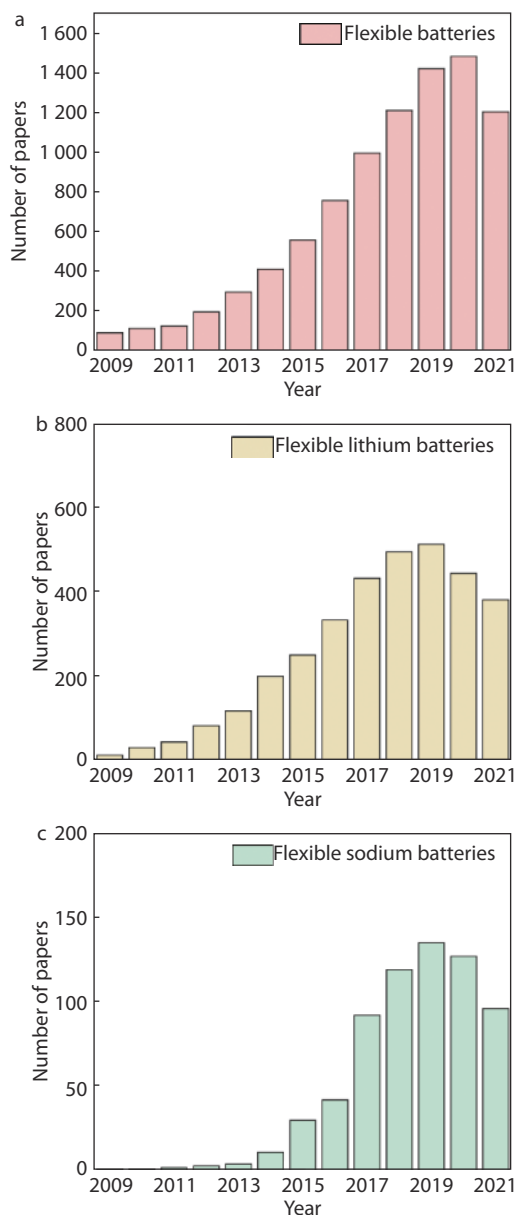


Fig. 2 The trends of "flexible battery", "flexible lithium-ion battery" and "flexible sodium-ion battery" in the past 10 years after "Web of Science".

graphene aerogels and other active material composites are used to prepare flexible electrodes directly by certain methods (electrostatic spinning^[25–27], cross-linked polymerization^[28], vacuum extraction^[29], gel drying or compression^[30,31]). Specifically, Figure 3 lists eight common methods of preparing flexible electrodes for flexible sodium-ion batteries. In addition, the electrochemical properties and synthesis strategies of flexible electrode materials prepared *via* metal substrates, carbon cloth substrates, carbon nanotubes, 2D graphene, 3D graphene aerogels and organic composites were presented in Table 1.

Due to its structural stability and high conductivity, it can be used as a construction platform for flexible batteries. By directly growing or depositing the active material on the conductive carbon cloth, the transport path of electrons and ions

in the flexible material can be effectively increased. Although carbon cloth-based materials are not dominant in mass-energy density, they have great flexibility and conductivity in flexible sodium ion energy storage devices, and have unlimited possibilities. In general, the advantages and disadvantages of different substrates of flexible electrodes are different. Graphene and carbon cloth have great advantages in terms of conductivity and flexibility, but operability and cost are urgent problems to be solved; compared with carbon cloth, CNFs and CNTs have lower mechanical elasticity, but through low operability electrospinning Silk technology can encapsulate various active materials on the surface of CNFs/CNTs or active materials; although metal-based materials have high electrical conductivity, their weak mechanical flexibility and stability are still difficult to solve; Polymeric flexible thin film electrodes based on cross-linked polymerization of organic molecules have excellent flexibility. However, the low electrical conductivity and high solubility of polymeric organic materials in conventional non-aqueous electrolytes currently limit their development^[17].

2.2 Challenges in the evaluation of flexible sodium ion batteries

A fair comparison in terms of the 'flexibility' and 'wear resistance' of the various flexible electrode materials or flexible sodium ion devices remains an issue. Due to these limitations, most of the reported work has typically used simple manual bending, torsion and tensile tests to determine mechanical flexibility and durability, without obtaining quantitative data relating to modulus, tensile strength, etc., which seems somewhat arbitrary.

2.2.1 Mechanical evaluation of electrode materials

It is necessary to establish a systematic set of criteria to assess the mechanical flexibility and durability of flexible sodium ion batteries. For the free-form factor, shape deformations such as bending, compression, twisting and stretching need to be ensured. Flexibility can be assessed by measuring the bending angle or radius, folding into a crane, rotating into a circle, percentage of extension length or tensile strain as well as compressive strain^[14]. In addition, the degradation of the device's properties under different deformation conditions needs to be measured. While the degree of deformability or performance retention depends on the target application, it needs to be standardized for application-oriented unit designs. For example, the all-round flexibility of an energy storage device is considered to be the dynamic stability in the case of bending > 180 degrees, folding > 1000 times, torsion > 125 turns/degree, tension > 50% compression. The inherent flexibility of electrode materials is the basic prerequisite for good deformation of flexible sodium-based energy storage devices.

Figure 4b, d shows the stress-strain curves by testing the C-frame and MoS₂@CF samples^[23]. It can be seen that MoS₂@CF has a high Young's modulus for the same stress change (from 20 kPa for C-frame to 65 kPa for MoS₂@CF). This demonstrates the excellent resilience properties of MoS₂@CF. The compression stress-strain curves for the framework obtained a larger hysteresis loop for MoS₂@CF compared to the compression stress-strain curve, indicating an increased dissipation of mechanical energy in MoS₂@CF due to the bending of

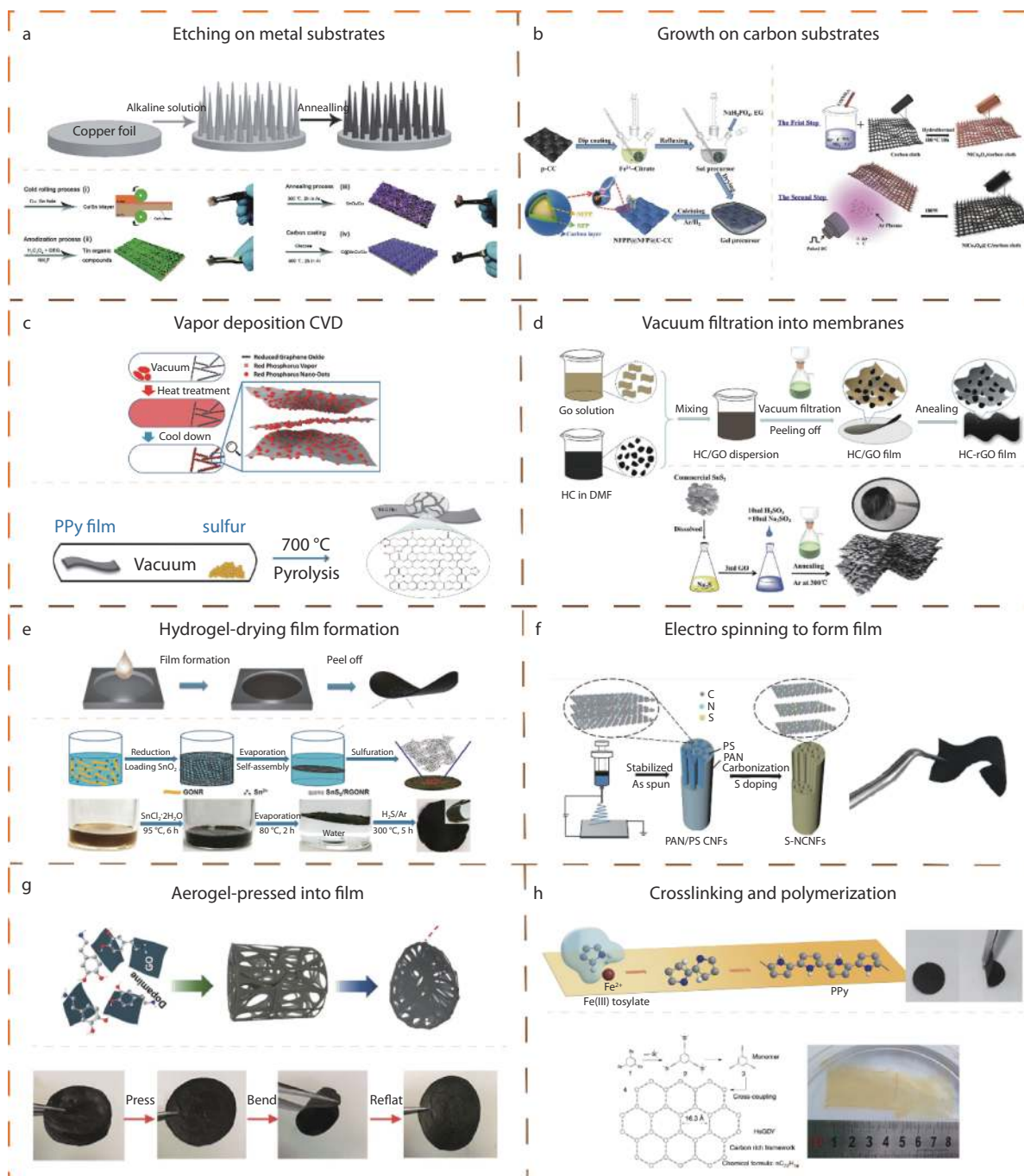


Fig. 3 Preparation of electrode materials for flexible sodium ion batteries: (a) Etching on metal substrate. Reproduced with permission.^[12] Copyright 2018, Elsevier. (b) Grown on carbon substrate. Reproduced with permission.^[20] Copyright 2017, Elsevier. (c) Vapor deposition Vacuum into membranes. Reproduced with permission.^[32] Copyright 2017, American Chemical Society. (d) Vacuum filtration into membranes. Reproduced with permission.^[33] Copyright 2018, Elsevier. (e) Hydrogel-drying film formation. Reproduced with permission.^[34] Copyright 2017, American Chemical Society. (f) Electrospinning to form film. Reproduced with permission.^[26] Copyright 2018, Wiley-VCH. (g) Aerogel-pressed into film. Reproduced with permission.^[35] Copyright 2018, Wiley-VCH. (h) Crosslinking and polymerization. Reproduced with permission.^[36] Copyright 2017, Springer Nature.

the cell walls in the porous microstructure and initial friction. When the compression tests were repeated for several cycles (1st, 10th and 20th, Figure 4c, e), all samples showed good overlapping stress-strain curves, demonstrating good reproducibility. Continuous photographs of the MoS₂@CF samples under uniaxial compression are shown in Figure 4f, g. The mechanical analysis of a single flexible electrode material is

mainly to evaluate its electrical conductivity and structural cracks under deformation conditions. To demonstrate the flexibility of the MoS₂/C NSA electrode, its electronic conductivity was measured by the four-probe method under different mechanical deformation conditions. Figure 4h shows that the conductivity of the MoS₂/C NSA electrode is approximately 8.8 S cm⁻¹ without any significant change even after

Table 1. Preparation method of flexible electrode materials and their electrochemical properties. Note: The synthesis method is replaced by the letters a-h inside Figure 3.

Ref	Flexible electrode	Synthesis method	Cycling stability (mA h g ⁻¹)	Practical capacity (mAh g ⁻¹)
Metal Cu/Ti foil substrate				
[12]	CuO /Cu foil	a	290.6 (0.2 A g ⁻¹ , 450 cycles)	640 (0–3.0V, 0.2 A g ⁻¹)
[37]	SnO ₂ /Cu foil	a	326 (0.2 C, 200 cycles)	232 (0–2.0V, 2C)
[37]	C@SnO _x /Cu fo	a	510 (0.1 A g ⁻¹ , 100 cycles)	300 (0–2.0V, 1 A g ⁻¹)
[38]	V ₂ O ₅ array/Ti foil	a	95 (0.25 A g ⁻¹ , 500 cycles)	120 (1.0–4.0V, 0.25 A g ⁻¹)
Carbon cloth substrate				
[39]	FPCC	b	88% (600 cycles)	123.1 (0–1.5V, 1 A g ⁻¹)
[18]	TiO ₂ /CFC	b	148.7 (1 A g ⁻¹ , 2000 cycles)	155 (0.01–3.0 V, 5A g ⁻¹)
[19]	L-NT0 NW@CC	b	100.6 (3C, 300 cycles)	211.9 (0.01–2.5 V 1C)
	MoO _{3-x}	b	92% (1 A g ⁻¹ , 2000 cycles)	156 (1.0–4.0 V, 0.1 A g ⁻¹)
[20]	NiCo ₂ O ₄ @C/CC	c	535.47 (0.5 A g ⁻¹ , over 100 cycle) 318 (5 A g ⁻¹ , 700 cycles)	749.9 (0–3.0V)
[21]	Ni ₃ V ₂ O ₈ /CC	b	233.3 (0.5 A g ⁻¹ , 275 cycle)	675.0 (0–3V, 0.5A g ⁻¹)
[40]	Sb ₂ O ₃ /CC	b	900 (0.05 A g ⁻¹ , 100 cycles)	1055 (0–3.0V, 0.05 A g ⁻¹)
[22]	ZnO-Co ₃ O ₄ /CC	b	265 (2 A g ⁻¹ , 400 cycle)	684 (0.01–3.0 V, 0.2 A g ⁻¹)
[23]	MoS ₂ NSAs	---	240 (1 A g ⁻¹ , 500 cycle)	252 mA h g ⁻¹ at 0.5 A g ⁻¹
[41]	MoS ₂ /C-NSA	a, b	320 (1 A g ⁻¹ , 1500 cycles)	433 (0.4–3.0 V, 0.2 A g ⁻¹) 232 mAh g ⁻¹ at 10 A g ⁻¹
[42]	CC@CN@MoS ₂	b	265 (1 A g ⁻¹ , 1000 cycles)	650 (0–3.0V, 0.2 A g ⁻¹)
[43]	MoSe ₂ @CC	b	202 (at, 1000 cycle)	452.6 (0–3.0V, 0.2 A g ⁻¹)
[44]	FeS@C/carbon cloth	b	365 (0.15 C, 100 cycle)	463 (0.5–3.0V, 0.15 A g ⁻¹)
[45]	FeP NAs/CC	b	548 (0.2 Ag ⁻¹ , 100 cycle)	829 (0.01–3.0V, 0.1 A g ⁻¹)
[46]	C-VOCQD	b	80% (60 C, 200 cycles)	321 (3.5–1.5 V, 0.3 C) 133 mA h g ⁻¹ at 60 C
[47]	FeFe(CN) ₆ /CC	b	≈40 (1200 cycles, at 1C)	82 mA h g ⁻¹ at 0.2C ≈50 mA h g ⁻¹ at 10C)
Carbon nanofibers based flexible self-supporting electrode				
[25]	NCNFs	f	203.1 (1000 cycles, 1 A g ⁻¹)	349.1 (0.01–2.5 V, 50 mA g ⁻¹)
[26]	S-NCNF	f	187 (2000 cycles, 2 A g ⁻¹)	132 (0–3.0V, at 10 A g ⁻¹)
[48]	NSCNIFs	f	90.8% (6000 cycles, 10 A g ⁻¹)	147 (0.01–3.0V, 10 A g ⁻¹)
[49]	Hu CP/g-C ₃ N ₄	f	110 (42000 cycles, 1 A g ⁻¹)	---
[27]	CuCo ₂ O ₄ @C	f	314 (1000 cycles, 1 A g ⁻¹)	296 (0–3.0V, 5A g ⁻¹)
[50]	2-CuO@C	f	401 (500 cycles, 0.5 A g ⁻¹)	250 (0–3V, 5A g ⁻¹)
[51]	MnS@CNF	f, b	220 (200 cycles, 20 mA g ⁻¹)	87 (0.01–3.0 V, 1A g ⁻¹)
[52]	SnS	f	327.5 (500 cycles, 5 A g ⁻¹),	782.8 (200 mA g ⁻¹)
[53]	CoS ₂ @MCNF	f, b	315.7 (1000 cycles, 1 A g ⁻¹)	209 (0.01–3.0 V, 10A g ⁻¹)
[54]	CoSe ₂ /CNFs	f	370 (2 A g ⁻¹ after 1000 cycles)	224 (0–3 V, 15 A g ⁻¹)
[55]	(NiS ₂ ⊂ PCF)	b	275 (5000 cycles, 5 C)	679 (0.01–3.0 V, 0.1 C) 245 (0.01–3.0V, 10C)
[56]	MoS ₂ /CNFs	f	283.9 (600 cycles, 0.1 A g ⁻¹)	381.7 (0.01–3.0 V, 0.1 A g ⁻¹) 246 (0.01–3.0 V, 1 A g ⁻¹)
[57]	MoS ₂ /CNFs	f, b	260 (2600 cycles, 1 A g ⁻¹)	410 (0.01–3.0 V, 1 A g ⁻¹)
[58]	MoS ₂ /CNFs	f, b	282 (600 cycles, 1 A g ⁻¹)	412 (0.01–3.0 V, 1 A g ⁻¹)
[59]	E-MoS ₂ /CNFs	f, b	241 (700 cycles, 1 A g ⁻¹) 104 (3000 cycles, 20 A g ⁻¹)	319 (0.01–3.0 V, 50 mA g ⁻¹) 222 (0.01–3.0 V, 1 A g ⁻¹)
[60]	ReS ₂ /N-CNFs	f, b	245 (800 cycles, 0.1 A g ⁻¹)	456 (0.01–3.0 V, 0.1 A g ⁻¹)
[54]	CoSe ₂ /CNFs	f	370 (1000 cycles, 2 A g ⁻¹)	224 (0.01–3.0 V, 15 A g ⁻¹)
[61]	MoSe ₂ /HPCFs	f	234.1 (1500 cycles, 1 A g ⁻¹)	326.3 (0.01–3.0 V, 0.1 A g ⁻¹) 276.7 (0.01–3.0 V, 1 A g ⁻¹)
[62]	Na ₃ V ₂ (PO ₄) ₃ /C	f	100% (100 cycles, 0.1 C)	97 (2.8–4.0 V, 1 C)
[63]	Na _{3.12} Fe _{2.44} (P ₂ O ₇) ₂	f	95.1% (100 cycles, 1 C) 93.6% (200 cycles, 6 C)	97 (1.6–4.0 V, 1 C) 80 mA h g ⁻¹ , 6)
[64]	Na _{2+2x} Fe _{2-x} (SO ₄) ₃ @PCNF	f	95.2% (500 cycles, 40C and 5C)	2.0–4.0V
2D graphene-based flexible electrode				
[64]	ROGP	d	Almost 100 (500 cycles, 5 A g ⁻¹)	183 (0.01–2.5 V, 0.1 A g ⁻¹)
[65]	Graphene	d	195 (50 cycles, 50 mA g ⁻¹)	111 (0–3.0V, 1000 cycles, 1A g ⁻¹)
[66]	FNGP	e	56 (5000 cycles, 1A g ⁻¹)	203 (0.01–3.0V, 50 mA g ⁻¹)
[33]	HC-RGO	d	200 (500 cycles, 0.5A g ⁻¹)	372.4 (0.01–3.0V, 30 mA g ⁻¹)
[67]	3D NTO/GP	d	---	240 (0.01–2.5 V, 0.2C)
[68]	GO/CuS film	d	228.7(100 cycles, 0.1C)	96.8 (0.01–3.0 V, 6 C)

Table 1 (continued)

Ref	Flexible electrode	Synthesis method	Cycling stability (mA h g ⁻¹)	Practical capacity (mAh g ⁻¹)
[34]	SnS ₂ -RGONRP	e	255 (1500 cycles, 5 A g ⁻¹)	244 mAh cm ⁻³ , 10 A g ⁻¹)
[69]	SnS ₂ /S-rGO	d	300 (400 cycles, 200 mA g ⁻¹)	223 (0.005–3 V, 4 A g ⁻¹)
[70]	SnS ₂ @GNA	b	378 (200 cycles, 1200 mA g ⁻¹)	348 (0–1 V, 3 A g ⁻¹)
[32]	P@RGO	e	914 (300 cycles, 1593.9 mA g ⁻¹)	135.3 (0–3.0 V, 47.8 A g ⁻¹)
[71]	P/CFs@RGO	e, f	725.9 (55 cycles, 50 mA g ⁻¹)	406 (0–2 V, 1 A g ⁻¹)
[72]	RP/rGO flexible film	f	1625 (200 cycles, 1 A g ⁻¹)	679 (0–2.0 V, 6 A g ⁻¹)
[73]	NVP/CN-GO	d	83% (200 cycles, a 1 C)	87.4% (2.5–4.1 V, 10 C)
[74]	GO/NNMO	d	80 (200 cycles, 1C)	68.4% (2.0–4.1V, 10 C)
3D graphene-based flexible electrode				
[75]	3DG/FeS@C aerogel	g	632 (80cycles, 100 mA g ⁻¹)	152.5 (0.01–3, 6A g ⁻¹)
[76]	PBGA	g	214 (100 cycles, 85 mA g ⁻¹)	-----
[31]	N-GF	g	594 (150 cycles, 500 mA g ⁻¹)	852.6 (0.02–3.0V, 0.5 A g ⁻¹)
[77]	MoS ₂ @GF	c	290 (50 cycles, 100 mA g ⁻¹)	172 (0.01–3.0 V, 0.2 A g ⁻¹)
[78]	GVG	c	110 (1500 cycles, 18 A g ⁻¹)	306 (1.5–3.5V, 0.1A g ⁻¹)
[30]	GF/CNTs@SnO	c	540 (600 cycles, 0.1 100 mA g ⁻¹)	580 (0.01–3.0 V, 0.1 A g ⁻¹)
[79]	NEPP@rGO	e	62.3% (6000 cycle, 10C)	35 (200C) 128 (0.1C)
[80]	NVOF/rGO	e	83.4 (2000 cycles, 30 mA g ⁻¹)	70.3 (2.5–4.5V, 100C)
Organic flexible electrode				
[81]	PANS/C	h	118 (200 cycles, 100 mA g ⁻¹)	123 (1.8–3.7 V, 0.1A g ⁻¹)
[82]	PPy films	h	149.1 (after 1000 cycles, 10C)	93.8 (0–3.0 V, 20 C)
[83]	NS–Ppy/film	h	357.2 (2000 cycles, 2 A g ⁻¹)	155 (0–3.0 V, 1 A g ⁻¹)
[36]	HsGDY	h	360 (1000 cycles, 1 A g ⁻¹)	650 (0–3.0 V, 0.1 A g ⁻¹)
[84]	graphene/poly	g	71.4% (1000 cycles, 0.5 C)	72 (1.2–2.8 V, 5 C) 157 (0.1 C)
[85]	3D graphene/polyimide	g	80.4% (1000 cycles, 1000 mA g ⁻¹)	213 (1.5–3.5V, 50m A g ⁻¹)
[35]	polydopamine@GA	g	=0% (1000 cycles, 0.01A g ⁻¹)	210 (1.3–4.25V, 0.05 A g ⁻¹)
[28]	Polydopamine FWNTs	e, d	-----	109 (2.5–4.1V)

1000 bending cycles^[41]. There is still no significant change after the bending cycle. This value is approximately 11 times higher than the value obtained with pure MoS₂/C NSA (approx. 0.8 S cm⁻¹). Such excellent flexibility and high conductivity make MoS₂/C NSAs promising anodes for elastic cells. Figure 4i further demonstrates the excellent cycling stability of MoS₂/C NSAs in flexible sodium-ion half-cells prepared by bending tests (capacity retention of ~94% over 200 bending cycles). In addition, the assembled flexible half-cell can also power white light-emitting diodes (LEDs) in both flat and 15° bending conditions (Figure 4j and k). The brightness of the LED remains unchanged even after 200 bending cycles (Figure 4l). Figure 4m shows digital photographs of the N-CNF at different bending angles, which means that the N-CNF electrode has good flexibility and mechanical integrity, which allows it to be freely folded and shaped into any desired form^[87], the tensile strain of the N-CNF is 1.689% and the tensile stress is 0.875 MPa (Figure 4n). The strength and robust structure of this film ensure the mechanical stability of the electrodes and the stability of their cycling properties.

2.2.2 Mechanical and electrochemical analysis of device deformation

It is a challenge to accurately assess the electrochemical capability of flexible sodium ion batteries (e.g. charge/discharge plateau, rate performance, cycling stability, energy density and power density) under various flexible testing methods (e.g. stretching, compression, bending, folding, twisting). For non-flexible Li-ion batteries, which are already widely used in industry, a common strategy used to achieve the total energy of a single cell system and improve space utilization is to stack multiple poles.

This strategy is clearly not feasible for flexible batteries, as the multiple components of the battery (cathode, anode, diaphragm, electrolyte, packaging material) lead to voids and damage at multiple interfaces when being bent, which greatly affects the flexibility of the battery. In recent years, many published articles on flexible sodium ion full batteries have not provided enough information regarding the testing and evaluation of flexibility, and there are no uniform standards. Furthermore, in some articles, the cathode (anode) material matched to the flexible base anode(cathode) material in the full cell is not flexible; it remains a conventional coating on a metal foil. Most of their flexibility tests are relatively simple, for example, a multimeter and a light bulb were used to test the electrochemical properties under simple bending conditions (Figure 5a–f). Such simple tests ignore many practical situations and do not fully reflect the specific flexibility of sodium ion batteries. In fact, current commercial copper foils can be as thin as 7 μm. If the cathode and anode are still coated by using the conventional coating process: only the active material needs to be applied to a very thin collector and the coating is thin enough to eliminate the need for laminations. The pouch cells produced by this method generally light up the bulb and have a stable voltage output even when being bent.

Guo et al.^[124] reported that cathode material (Na_{0.44}MnO₂) and anode material (NaTi₂(PO₄)₃) were mixed with a conductive agent and binder, respectively, and coated it on a lightweight flexible stainless steel mesh. The final ribbon flexible full battery can be lit in a bent state in a 1 M aqueous solution of Na₂SO₄ when connected in series. The capacity of the flexible ribbon cell after 100 cycles at different bending angles (45°, 90°, 135°, 180°) actually decays somewhat compared to

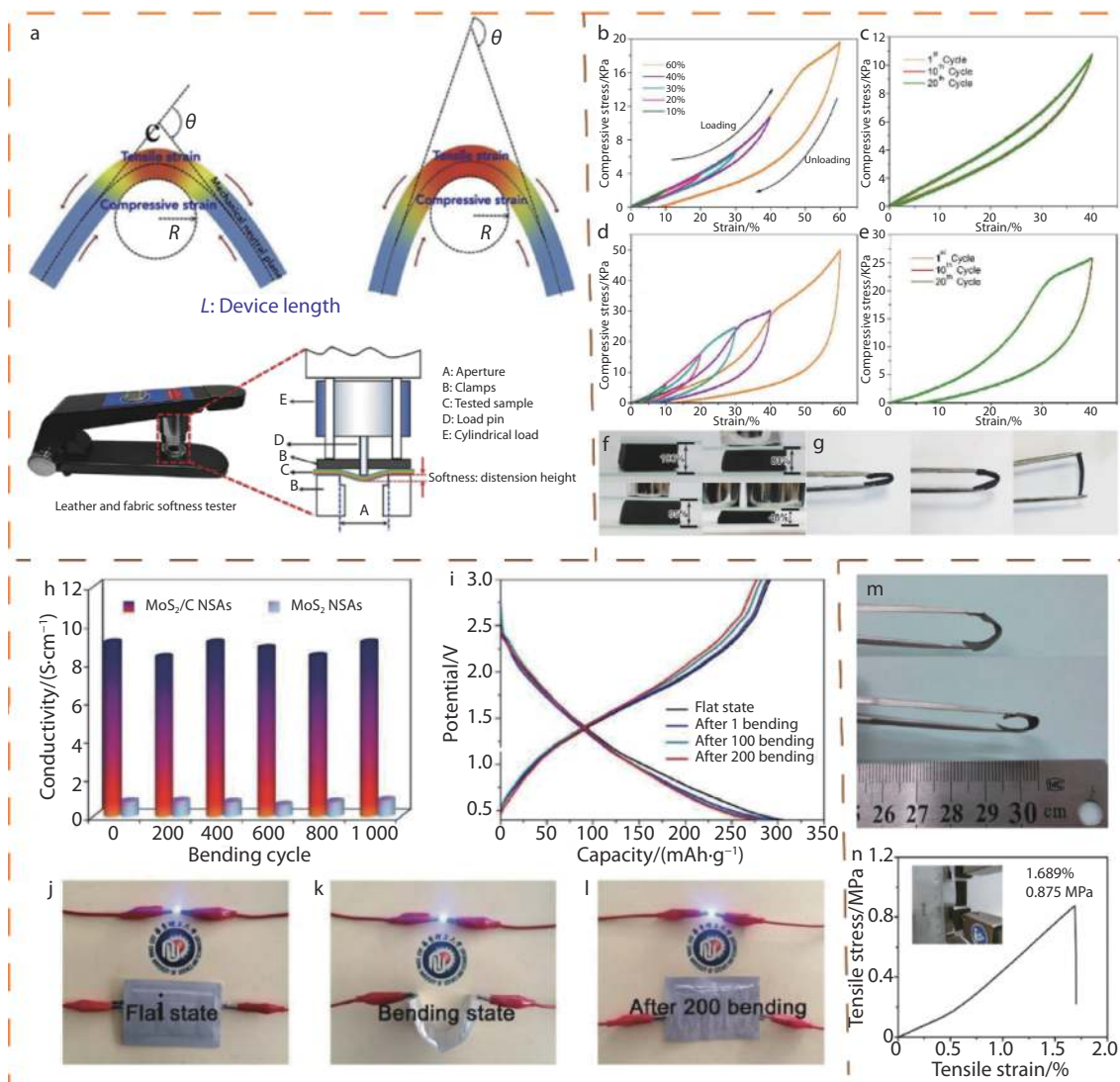


Fig. 4 a) Assessment tools for flexible fiber battery. Reproduced with permission.^[14] Copyright 2019, Elsevier. Compressive stress-strain curves of: b) C-framework and c) MoS_2/CF sample. Compressive stress-strain curves of several selected cycles of: d) C-framework and e) MoS_2/CF sample under 40% compressive strain condition. Sequential photographs of MoS_2/CF sample under: f) uniaxial compression and g) bending test. b-f) Reproduced with permission.^[23] Copyright 2020, Elsevier. h) The electronic conductivity values of MoS_2/C NSAs and MoS_2 NSAs during the bending test for 1000 cycles, i) the charge/discharge curves of the assembled MoS_2/C NSAs flexible battery under the flat state and after 1, 100, and 200 bending cycles, (j-l) a white LED connected to the flexible battery under the flat and bending states and after 200 bending cycles. h-l) Reproduced with permission.^[41] Copyright 2017, Elsevier. m) Digital photographs of N-CNF at different bending angles; n) stress-strain curve of N-CNF from tensile test. m,n) Reproduced with permission.^[87] Copyright 2016, Wiley-VCH.

that of before bending (Figure 5g). However, this battery did not compare the rate of capacity decay after 100 cycles without bending conditions. This makes it difficult to determine whether the capacity decay is due to repeated bending breaking the contact at each interface, increasing the impedance of the cell, or to cycling losses in the material itself. Sun et al.^[89] reported a flexible sodium ion anode based on self-supporting hematite nanoarrays ($\text{N-Fe}_2\text{O}_3/\text{CC}$) grown on carbon cloth. To verify its application in a practical flexible full cell, the prepared flexible anode was matched with a $\text{Na}_3\text{V}_2(\text{PO}_4)_3/\text{C}$ powder anode prepared by sol-gel method to make a full cell. This $\text{N-Fe}_2\text{O}_3/\text{CC}/\text{Na}_3\text{V}_2(\text{PO}_4)_3/\text{C}$ full cell exhibited a voltage plateau of 2.6 V and an energy density of 201 Wh kg^{-1} . To test the cycling stability of the battery under flexible conditions, the battery was first cycled 90 times at a

current of 116 mA g^{-1} and then the soft pack battery was folded 90° along the middle and the charge/discharge test continued, but a sudden slight increase in capacity was found (Figure 5h, i). This phenomenon requires further advanced characterization techniques to explain it. The CC-NVPO//PCC- TiO_2 dot-16 full cell made by Long et al.^[90] had a high mass loading (14.0 mg cm^{-2} for the cathode and anode, 5.0 mg cm^{-2} respectively), a first coulombic efficiency of 75.6% and an average discharge plateau of 2.45 V. Figure 5j shows the cycling stability test of the battery under bending conditions. After several continuous strain cycles at 0°, 90°, 180° and 0°, the capacity decay is negligible. This high quality loading design and cycling measurements to assess the performance of multiple continuous strain cycles provide a good reference for flexibility testing. Wang et al.^[88] prepared carbon nanofibre

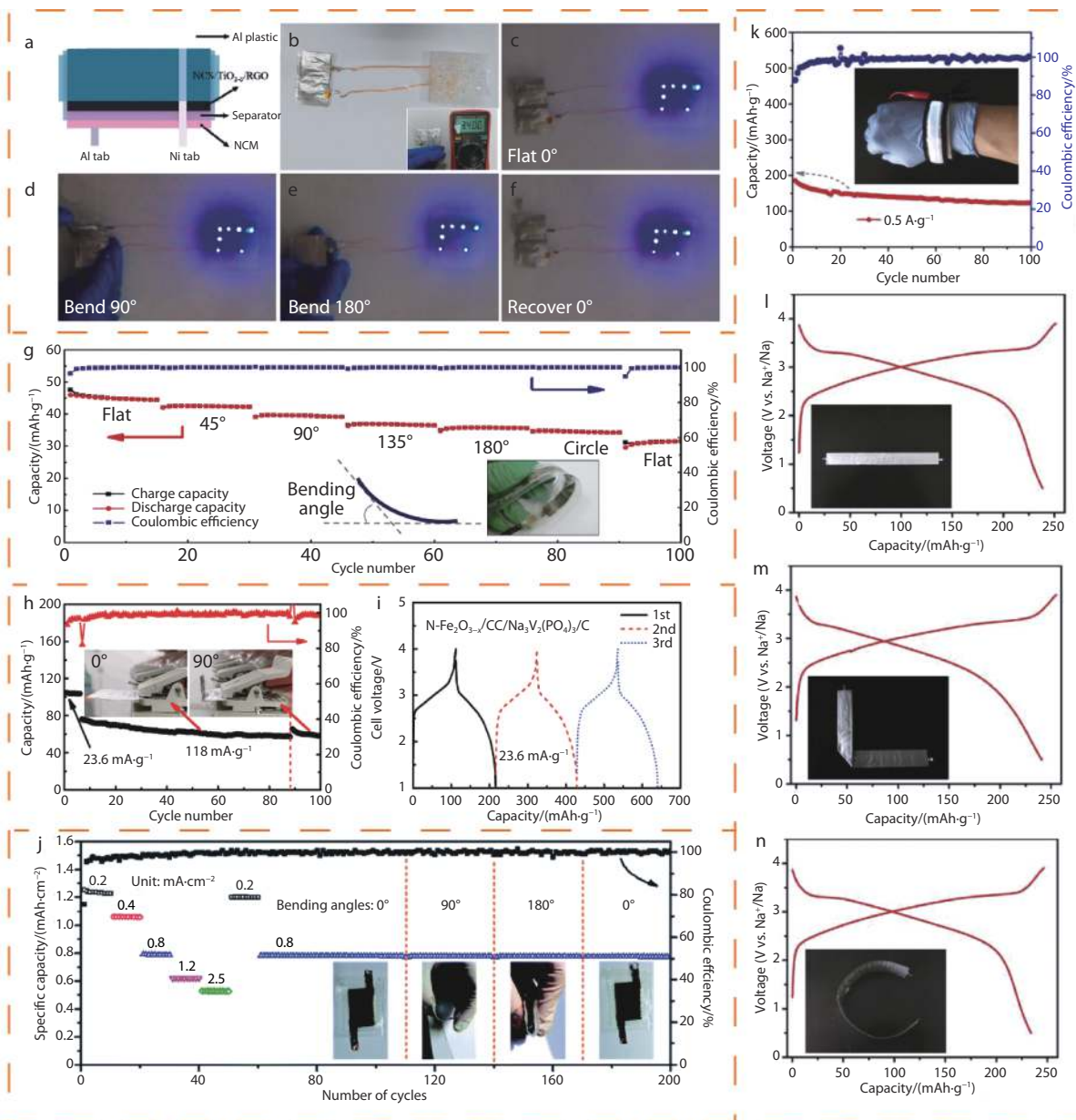


Fig. 5 (a) Schematic diagram of the soft-package NCS/TiO₂-δ/RGO/NCM battery. (b) Photograph of the soft-package battery and "Li" model LEDs (the inset shows the open-circuit voltage). (c-f) The NCS/TiO₂-δ/RGO/NCM battery was used to light "Li" model LEDs after bending at 0°, 90°, and 180° and recovering to 0°, respectively. a-f) Reproduced with permission^[86]. Copyright 2019, American Chemical Society. (g) Flexible Belt-Shaped Na_{0.44}MnO₂/NaTi₂(PO₄)₃@C Battery: Cycling profile under different bending conditions tested at a current density of 0.2 A g⁻¹. Inset is Photo profile of an as-prepared belt-shaped aqueous SIB. Reproduced with permission^[124]. Copyright 2017, Elsevier. (h) Galvanostatic profiles of full cell upon initial cycles. i) Cycle performance and bending test of full cell. h,i) Reproduced with permission^[89]. Copyright 2020, Wiley-VCH. j) Rate performance and flexible test of CC-NVPO k PCC-TiO₂ dot-16 full cell and inset shows the images of a soft-pack battery under different bending states^[87]. Reproduced with permission^[90]. Copyright 2019, Royal Society of Chemistry. (k) of the flexible full battery; a flexible LED bracelet lit by the prepared SIB full battery (inset). Galvanostatic charge/discharge profiles of the flexible battery under various shapes: flat state (j), 90° (m) and a cycle (n). k-n) Reproduced with permission^[88]. Copyright 2018, Elsevier.

films (NCFs) by using NH₃-treated coal tar pitch/acrylonitrile-based electrospun nanofibres. Strip flexible sodium ion full cells (NCFs//Na₃V₂(PO₄)₃@C) were prepared by matching Na₃V₂(PO₄)₃@C cathodes. After the cell was continuously charged and discharged at different bending angles (0°, 90°, 180°) (Figure 5k-n), it was still possible to observe almost no change in the charge/discharge curve of the cell, with a stable charge/discharge plateau observed between 3.3 and 2.2 V.

This holds great promise for future applications in flexible bracelet electronics.

Several of the above flexible full batteries have only been tested for charge and discharge cycles under simple bending conditions. We must be fully aware that there are still many irresistible factors that constrain the development of flexible testing and evaluation of sodium ion batteries. (1) The loading of different electrode materials and the size of the cell

shape can affect the results of flexibility testing. (2) The manufactured flexible material may not be very homogeneous (e.g. cracks, scratches, particles, gaps) easily causing stress concentration and the actual stress distribution during bending may not be uniform. (3) The bending angles considered in current bending tests do not allow comparison of strain changes in cells of different sizes, and better variable curvature should be used to measure this. (4) Traditional manual bending tests can cause unpredictable wear and unexpected changes in strain cycles. So, it is better to use automated test procedures by ideal test equipment to maintain the battery unit integrity under controlled strain direction, strain intensity and strain rate. In addition, flexibility testing cannot simply be a matter of measuring the conditions before and after a single bending process. It should be necessary to assess the cycling stability of the cell over several successive strain cycles, to predict changes in the cell interface during bending, e.g. to test the change in impedance of the cell during dynamic bending and to compare the capacity degradation before and after a long cycle with and without strain conditions.

2.3 Challenges for the application of flexible sodium-ion batteries

2.3.1 Cycle/Calendar Life

When studying the cycle life or calendar life of non-flexible sodium ion batteries, it is generally necessary to focus only on the properties of the battery material itself, such as (i) collapse of the material microstructure; (ii) irreversible loss of active material from the electrode material; (iii) continuous increase in interfacial impedance leading to increased polarization; (iv) cracking of secondary particles of the active material; (v) decrease in conductivity due to contact shedding between the active and inactive materials; (vi) cell (vii) internal micro-reactions leading to gas production; (viii) incompatibility of the positive and negative electrodes of the cell leading to poor Coulombic efficiency, etc. As flexible sodium ion batteries were generally operated in a long-term stress environment, this leads us to consider the effects on the internal microstructure of the cell due to external environmental effects. For example, the device configuration, the compatibility of the components and the fatigue resistance of the entire device in relation to mechanical strength and wear resistance. The interfacial contact between the various components within the entire device will be significantly affected under long-term stress, e.g. the decomposition of electrolyte salts could limit the shuttling of ions through the electrolyte leading to irreversible degradation of performance. In addition, the mechanical strength and wear resistance of the outer packaging will even affect the possible leakage of the electrolyte. Further development of advanced flexible sodium ion batteries requires careful analysis of the external and internal causes of failure of flexible batteries. This requires further design of mechanically stable structures, the exploration of new materials with long-term mechanical strength and the application of effective encapsulation layers.

2.3.2 Energy/power density

In the quest for high energy and power density batteries, the search for new electrodes and active materials with low weight, high conductivity and high electrochemical properties is a promising strategy. As for the preparation of flexible

sodium ion batteries, the main approach is to improve electrode materials and device structure. The electrode materials with high specific capacity are considered to be a prerequisite for the development of high energy densities. However, flexible substrates that do not have the capacity contribution in the electrode will reduce the energy density of the whole device to some extent, which requires the development of thin substrates or active substrates with a capacity contribution if possible. This aspect is considered to be more promising for flexible negative electrodes, as carbon materials derived from carbon nanotubes, graphene, carbon cloth and carbon nanofibers have some sodium storage properties.

In addition, sodium ion batteries with good mechanical flexibility can also directly regulate the external macrostructure of the device. For planar, flexible sodium ion batteries with more layers of monolithic cells tends to increase the energy density of the system. The increase in the number of layers of cells then inhibits the bendability of the device and even affects the compatibility of different electrode materials and electrolytes. The design of small diameter fiber cells, or the integration of numerous micro cells in series and parallel onto bendable building blocks is also considered a common design strategy for flexible sodium ion batteries today.

2.3.3 Flexibility and Biocompatibility

Flexibility and biocompatibility are core elements of flexible sodium ion batteries, which have a direct impact on the first-time user experience.

For planer-shape flexible sodium ion batteries, the thickness of the stack determines the energy density and flexibility. The use of in-plane micro cells or array or island-bridge arrangements can to some extent alleviate the flexibility limitations of the electrode material. It is mainly from a mechanical point of view to transfer the stress deformation between the electrode material and the electrolyte. The flexibility of flexible cells with fiber shapes depend to a large extent on the diameter of the entire device. When the diameter is made as small as possible, for example, it is possible to use fibrous cells with a diameter in the hundred-micron class or even smaller for weaving/woven ones, so that the dense and flexible effect can be achieved. However, the currently reported thickness of fibrous cells is far from satisfactory as their complex structure consists of several integral components including electrodes, electrolyte and diaphragm/encapsulator, as their superimposed effect inevitably increases the overall volume and thickness. Other challenges such as active material dissolution, component adhesion, electrolyte leakage and dilution should also be carefully considered. As a result, most laboratory studies only focus on the performance of centimeter-scale fiber-shape cells as a demonstration, but this approach does not reflect the real-world value of practical applications. As devices elongate, they will become significantly more difficult to be manufactured. With the development of 3D technology, the direct 3D printing of fiber batteries with coaxial structures is considered to be one of the most promising technology for future weaveable flexible batteries.

2.3.4 Safety

The safety of flexible sodium ion batteries is essential for commercialization of the devices. This includes various factors such as the structural stability of all device components, environmental influences, leak-free operation as well as

thermal and chemical stability. Currently, the main concern is cell encapsulation, electrolyte permeation and separator, which are closely related to safety issues. For encapsulation, polymers such as heat shrink tubing, PET film and silicone rubber have been widely used as flexible encapsulation layers, but their capability to keep out water and oxygen is not as good as it could be. This is because flexible batteries also require a certain level of water resistance in the wearable sector. For organic-based electrode solutions, the water-free environment inside the cell is related to the cycling life of the battery. The internal construction of flexible batteries is still two electrodes separated by an intermediate separator to avoid short circuits. Most of the cells reported in the laboratory use GPE as the separator, but the limited mechanical strength of the polymer electrolyte is still not sufficient for practical requirements, especially when large deformations are applied. For future wearable applications, the establishment of an effective spacer will ensure long-term stability. A final issue is the permeation of the electrolyte fluid, where contact between the flexible battery and the human body is inevitable in the field of flexible wearables. Although we propose to achieve tight encapsulation, given the inadequacy of existing technologies, the outer packaging will inevitably break due to fatigue effects during long-term mechanical stress, which will lead to the leakage of some toxic, corrosive and flammable electrolyte or electrode materials. So, the use of non-toxic electrode materials and mild aqueous electrolytes is considered to be a solution. In addition, replacing conventional organic electrolytes with gel polymers or solid electrolytes is also considered as a possible solution to avoid electrolyte leakage. Furthermore, thermal runaway has been a well-known problem for high power non-protonic batteries, especially during ultra-fast charging and discharging or under hazardous conditions such as short circuits and overcharging; therefore, effective thermal management is necessary to avoid overheating and any short circuits. The structure of flexible electrochemical energy storage devices is very complex because each factor is coupled to the other and there can be considerable influence between them. Therefore, understanding and accurately factors of material and device design can provide durable, comfortable and versatile electrochemical performance for flexible sodium ion battery systems.

2.3.5 Multifunctional integration

Multifunctional systems are key to broaden the range of applications for flexible sodium ion batteries. For example, stretchable, self-healing, transparent and self-charging functions being assembled in flexible sodium ion batteries is also a very promising direction for future research. In addition, many wearable devices with integrated biosensors can also be powered by flexible sodium ion batteries to detect a number of stress responses, such as electrochromic properties, photodetection, thermal reactivity, and freeze resistance. However, the construction of such a single device configuration is complex, involving an in-depth understanding of the working mechanisms at the intersection of scientific and technical perspectives from different fields, and requires a very fine design involving device assembly, compatible components and energy management.

3 Application of flexible sodium ion batteries

3.1 Component matching and optimization of flexible sodium ion full battery

Table 2 shows flexible sodium ion full cells after matching various cathode and anode materials, along with information about their flexibility testing, loading, cell structural design, plateau voltage, cycling stability and energy density. (An "*" in front of an electrode material indicates that the material is flexible; the absence of an asterisk indicates that the electrode material is still conventionally coated). We can see that only a few cathode or anode are flexible materials in the reported articles. So, future research on flexible sodium ion batteries should focus on how to correctly match different cathode and anode materials and different types of electrolytes, which not only meet the requirements of high voltage, high multiplicity, high energy density and long cycle stability, but also meet flexibility assessment criteria.

3.1.1 Traditional Flexible Sodium-Ion Batteries

In non-flexible sodium ion batteries, the most commercially promising cathode materials are laminate oxide, polyanionic and Prussian blue analogues; while the most commercially promising anode materials are hard carbon and modified soft carbon materials; therefore, flexible electrodes based on these most commercially promising cathode and anode materials are considered to be the most promising one in the field of flexible sodium ion batteries. Wu et al.^[112] used commercially available cotton carbon cloth (CC) as a substrate for flexible anodes and cathodes. The binder-free, self-supporting flexible cathodes (FCC@NPB) were prepared by growing Prussian blue microcubes on flexible CC (FCC) (Figure 6a). FCC and FCC@NPB were assembled as anode and cathode, respectively; to form Na ion full cells (FCC//FCC@NKPb) (Figure 6b). The electrochemical performance, mechanical flexibility and practicality of the FCC//FCC@NPB Na ion full cell were evaluated in coin cells and soft pouch batteries, respectively; and the results showed excellent multiplicative performance, cycling stability and significant flexibility (they can operate in different bending conditions) (Figure 6c, d).

Zhang et al.^[93] prepared hard carbon fiber membrane coated porous $\text{Na}_3\text{V}_2(\text{PO}_4)_3$ (NVP/HCF) cathodes by using hard carbon fiber paper (HCF) as a support frame and three-dimensional conducting network for flexible sodium-ion full battery (FSIFBs). Several different pre-sodiated anodes (PHCF, NaVOPO_4 , PGN/SiC/HCF) in different levels of electrolyte additives (0%, 5% FEC) were also investigated in a flexible sodium ion full cell, which exhibited good electrochemical performance. FSIFBs assembled with PGN/SiC/HCF anodes have smaller polarization and impedance, higher output voltage and rate performance compared to pre-sodiated HCF (PHCF) and NaVOPO_4 anodes (Figure 7a). In Figure 7b, the charge and discharge curves of NVP/HCF//PGN/SiC/HCF full cells are consistent at different bending angles. Figure 7c, d show the impedance before and after folding at 2.8 V. It can be seen that there is an anomaly: the impedance of the folded FSIFB is lower in the high and mid frequency region than the FSIFB before folding. This may be due to the fact that the cell creates the right tension during bending, allowing better contact between the active particles at the electrode interface

Table 2. properties of various sodium ion full batteries. Note: "*" indicates that the cathode (anode) electrode matched by the full cell is a flexible electrode.

Full cell(Anode//cathode)		Working potential	Flexibility Assessment			Cycling Performance specific capacity	Energy Density Wh kg ⁻¹ (A g ⁻¹)	Ref
			Light LED	Cycle test	Device structure			
*CNFs	*NaFePO ₄ @ CNFs	1.0–4.0 V	√	√	Pouch	87% (200)(0.5C)(1C=150 mA g ⁻¹)	168.1(0.5C)	[91]
*PGN/SiC/HCF	*BFCF-NVP/HCF	2.0–4.6 V (3.34V)	√	√	Pouch	—————	234.1 (0.5)	[92]
*Fe _{1-x} S@PCNWs/rGO	*NVP/rGO	0.1–3.0 V	√	√	Pouch	—————	—————	[93]
*Sb/rGO	*NVP/rGO	0.7–3.5 V	√	√	Pouch	—————	—————	[94]
*Na ₂ Ti ₃ O ₇ @N-GQDs	*Na ₃ V ₂ (PO ₄) ₃ @NC	2.0–3.8 V	√	√	Pouch	103.2 97.8% 230 cycle (0.5C)	273.5	[95]
*Carbon-networks/Fe ₇ S ₈ /graphene (CFG)	*Na ₃ V ₂ (PO ₄) ₃ @C	0.3–2.2 V	√	√	Pouch	1.42 mAh cm ⁻² at 0.3 mA cm ⁻²	144	[96]
*VO ₂ NS/CC	*Na ₃ (VO) ₂ (PO ₄) ₂ F(INVOF array/GF	1.0–4.0 V	√	√	Pouch	80% (220) 4C	212(312)	[97]
*NCFs	Na ₃ V ₂ (PO ₄) ₃ @C	0.5–3.9 V2.2–3.3V	√	√	Belt	68%(100)	—————	[25]
*k PCC- TiO ₂ dot -16	CC-NVPO	2.0–4.0 V	√	√	Pouch	—————	—————	[90]
*N-Fe ₂ O _{3-x} /CC	Na ₃ V ₂ (PO ₄) ₃ /C	2.5–4.0 V	√	√	Pouch	—————	201	[89]
*CoP ₄ /CF	Na ₃ V ₂ (PO ₄) ₂ F ₃ @Al	1.5–4.2 V	√	√	Pouch	81%(50)(100)	280 Wh/kg(0.1)	[98]
*CoSe ₂ /CNFs	Na ₃ V ₂ (PO ₄) ₃	0.01–3 V	o	√	Pouch	370 200 200	—————	[74]
*NCS/TiO _{2-x} /rGO	Na _{0.67} Fe _{0.3} Mn _{0.3} Co _{0.4} O ₂	1.6–4.2 V	√	√	Pouch	—————	128	[86]
*Bi ₂ S ₃ /3DNG	Na _{0.4} MnO ₂	3.5V	√	√	Pouch	—————	—————	[99]
*MnS@CNWs/rGO	Na _{0.7} MnO ₂	0.5–3.5 V	√	√	Pouch	—————	—————	[100]
*GN/NaTi ₂ (PO ₄) ₃ /GN	Na _{0.44} MnO ₂	2.0–4.0 V	√	√	Pouch	92.3%(30)	—————	[101]
*CNFs	*PTCDA/RGO/CNT	0.7–2.7 V	√	√	Pouch	—————	104.4	[102]
Sn(PVDF-HFP)	C(PVDF-HFP)	2.0–4.5 V	√	√	Pouch	—————	—————	[103]
Na CESS NVP	Na ₃ V ₂ (PO ₄) ₃	2.6–4.0 V	√	√	Fiber	—————	—————	[104]
NaTi ₂ (PO ₄) ₃ @C	*Na ₃ V ₂ (PO ₄) ₃ /CNF	0.4–2.0 V	√	√	Fiber	—————	123(20 mA/g)Vs cathode	[105]
*NVP@C@rGO,	*NVP @C-CC	0.7–2.4V	√	√	Pouch	67.3% (500) 5C	94 (50C)	[33]
*Na ₂ VTi(PO ₄) ₃ /CNFFs	*NVP@C@rGO	1.2–2.2 V	√	√	Pouch	47.8 86.6% (200)	—————	[106]
*NaTi ₂ (PO ₄) ₃ (NTPO@C)	*Na ₂ VTi(PO ₄) ₃ /CNFF	0.0–1.5 V	√	√	Pouch	83%(600)(40C,4C)	34(70 W/kg)	[107]
*CNT/NTPO@C hybrid fibers	*Na _{0.44} MnO ₂ (NMO)(Na ₂ SO ₄ electrolyte)	0–1.6 V	√	√	Fiber	60%(1000) 0.2 A g ⁻¹	23.8 mWh cm ⁻³	[87]
NGQDs-WS ₂ /3DCFFiber-shaped	*(CNT)/NMO(Na ₂ SO ₄ electrolyte)	0.0–1.6 V	√	√	Fiber	76%(100)(0.2 A g ⁻¹)	25.7 mWh cm ⁻³	[87]
*NaTi ₂ (PO ₄) ₃ @CNTF	Na _{0.44} MnO ₂ /nickel- foam	1.6–3.5 V	√	√	Fiber	58.1(100)(50)	—————	[108]
Na	*KNiFe(CN) ₆ @CNTF	0.0–1.5 V	√	√	Pouch	34.21 mAh cm ⁻¹	39.32 mWh cm ⁻³	[109]
*Ni ₂ P@PNC	*titania/rGO/CNTs hybrid fiber	0.0–3.0 V	√	√	Pouch	60.3%(2000)(85)	—————	[82]
HC SH/NaNO ₃	KNi ₁₁ Fe ₁₁ (CN) ₆ SH/NaNO ₃	0.1–1.5 V	x	√	Self-Healable	—————	—————	[110]
Na	PB @ GO @ NTC	2.2–3.7 V	√	√	Fiber	—————	—————	[111]

and thus improving the charge transfer. Alternatively, the folded cathode and label are closer together and have better contact, resulting in a lower resistance of the whole cell. The graphs show that the battery pack has a long cycling stability (77.8% capacity retention at 0.5A g⁻¹ for 2905 cycles). In addition, Figure 7e-i shows that the cell can light up a light bulb under bending conditions in water. This article provides an effective way to develop flexible, low-cost electrode materials with excellent electrochemical properties. In addition, the selection and matching of cathode and anode materials for flexible sodium-ion full batteries and the kinetic studies under bending conditions are presented, which are important references for the optimal design of flexible sodium ion full batteries.

3.1.2 Symmetrical NASICON battery

For the high-rate, long-cycling flexible sodium-ion batteries, the most studied is the NASICON electrode material. The main advantages of this electrode material are high ion con-

ductivity and structural stability^[114]. NASICON electrode materials can be cross-linked with carbon nanofibers or carbon cloth to form a three-dimensional macroporous frame (as a robust electronic pathway and a flexible buffer to accommodate volume changes resulting from the repeated Na⁺ insertion/extraction). It has a robust electronic pathway, and carbon nanofibers or carbon cloth as a flexible buffer can adapt to the volume change caused by repeated insertion/extraction of Na⁺. For example, NVP@C-CC was reported by Guo et al.,^[113] which exhibits good cyclability (82.0% capacity retention over 2000 cycles at 20 C) and high rate capacity (96.8 mA hg⁻¹ at 100 C and 69.9 mA hg⁻¹ at 200 C) for sodium half cells (Figure 8a-f). The vanadium-based electrode has two voltage plateaus at 3.4V and 1.6V, which are the characteristic voltage positions of the valence changes of V³⁺/V⁴⁺ and V²⁺/V³⁺, respectively; therefore, this phosphate can be used in both cathode and anode materials, with theoretical capacities of 117 mAh g⁻¹ and 50 mAh g⁻¹, respectively. If both of

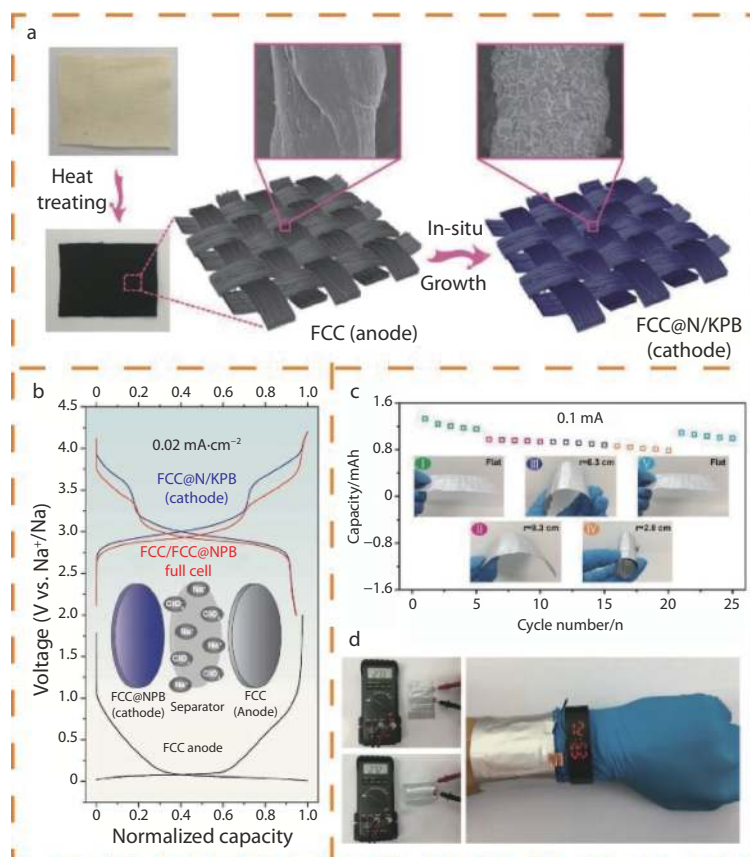


Fig. 6 a) The schematic illustration of the formation process for the flexible binder-free FCC anode and FCC@N/KPB cathode. b) The GCD curves of FCC anode, FCC@NPB cathode, and FCC//FCC@NPB full cell at a current density of 0.02 mA cm^{-2} ; c) Cycling stability of the FCC//FCC@NPB at different bending states (the inset shows the flexibility with different mandrel radius) at a current of 0.1 mA ; d) Left: The voltage of FCC//FCC@NPB flexible pouch cell at the state of flat and bending; right: the application demonstration of commercial electronic watch by using the FCC//FCC@NPB flexible pouch cell as power supply^[112]. a-d) Reproduced with permission.^[112] Copyright 2019, Wiley-VCH.

the cathode and anode the flexible sodium ion full battery use the composite flexible material formed of this NASICON type material and a flexible substrate, it will have the advantages of ultra-high rate performance and low cost^[84,93–96]. In addition, symmetric cells are also very compatible with aqueous electrolytes (e.g. NaSO_4 , NaNO_3 , saline) very well. These batteries tend to have low voltages (typically 1–2V) and the water-based inorganic salt electrolytes have a relatively small voltage range, which is just right for the low voltage requirements. In addition, water-based electrolytes have the advantages of considerable ionic conductivity, non-toxicity and good biocompatibility. Dong et al.^[107] prepared a symmetric water-based rechargeable sodium ion battery using two $\text{Na}_2\text{VTi}(\text{PO}_4)_3/\text{C}$ nanofiber electrodes as the cathode and anode, respectively, and Na_2SO_4 as the aqueous electrolyte. As shown in Figure 8g–j the cross-linked nanofiber film can be easily twisted and bent in different arcs, showing its good flexibility. The cell exhibits a flat potential plateau at 1.2 V with a long-term high-rate cycling capability (with 83% capacity retention after 600 cycles between 40C and 4C rate). Thus, the flexible sodium ion full cell matched by symmetric flexible electrode material and aqueous electrolyte provides a new idea for designing an energy storage device with high rate, long cycle stability and low cost. And it will promote the development of energy storage batteries for mi-

croelectronics and implantable biomedical device.

3.1.3 All-Solid-State Flexible Battery

Solid and gel polymer electrolytes are considered to be the ultimate choice for future flexible sodium-metal full batteries with high voltage, high energy density and long cycling life due to their high potential window and good mechanical flexibility. The current challenge for solid electrolytes is to improve ionic conductivity and to address the high impedance caused by interfacial problems. Several recent publications have greatly contributed to the development of flexible sodium ion solid polymer electrolytes. Yao et al.^[115] designed an advanced all-solid-state sodium cell ($\text{NVP@C} \mid \text{PEGDMA-NaFSI-SPE} \mid \text{Na}$) which uses carbon coated $\text{Na}_3\text{V}_2(\text{PO}_4)_3$ (NVP@C) as the cathode and sodium metal as the anode (Figure 9a, b). The PEGDMA-NaFSI-SPE is the electrolyte. An effective integrated system of the electrolyte and anode was prepared using in-situ solvent-free polymerization, which greatly improved the ionic conductivity of the SSE ($\approx 10^{-4} \text{ S cm}^{-1}$ at RT) and enhanced the interfacial contact between the SSE and the electrode material. As Figure 10f demonstrates, the battery still maintained a stable voltage under different bending states. This flexible sodium ion battery still exhibited good cycling stability (reversible capacity of 106 mAh g^{-1} at 0.5 C rate for 535 cycles) when different deformation conditions were applied at different stages of constant current charge and discharge (Figure 9d). Furthermore, the impedance after

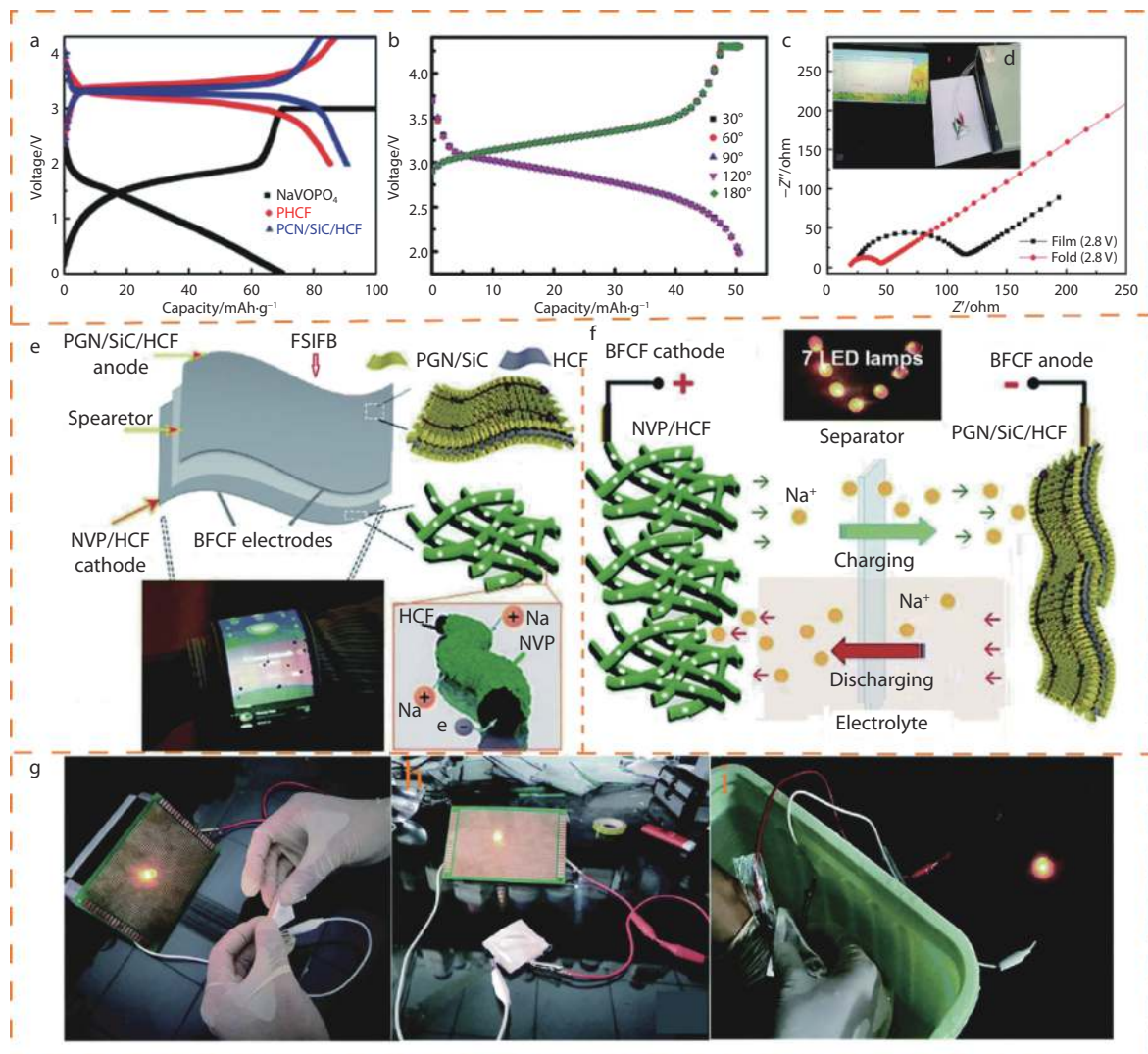


Fig. 7 a) Sodium storage performances of the pouch-type FSIFBs assembled with the BFCF-NVP/HCF cathode and the different anodes at different current rates of the cathode. b) Charge-discharge curves of the pouch-type FSIFB assembled with the BFCF-NVP/HCF cathode and the PGN/SiC/HCF anode at 5C after bending at different angles from 180 to 30. c) Nyquist plots of the FSIFB before and after being folded at a bending angle of 120 at 2C and 2.8 V. d) EIS test photograph of the bent pouch-type FSIFB. e) Schematic illustrations for the fabrication and microstructure of the flexible sodium-ion full battery (FSIFB) using the BFCF-NVP/HCF cathode and the PGN/SiC/HCF anode. f) Schematic diagram of the FSIFB. g) Bending and waterproofing tests on pouch type FSIFB. a-g) Reprinted with permission.^[91] Copyright 2016, Royal Society of Chemistry.

folding remains almost unchanged compared to the flat state as measured by EIS (Figure 9e). The battery showed almost no self-discharge after 3 months, demonstrating good long-term storage performance (Figure 9f). This work will provide a good direction for flexible sodium ion batteries with high voltage, long life and low self-discharge. Recently, a device that completely 3D printed solid fiber batteries may be an accelerator for the large-scale production of fibrous batteries in the future^[116]. The principle of the solid fiber battery printed by the device is shown in the Figure 9g, h. Specifically, the current collector, cathode material, electrolyte, anode material, and current collector are placed in different shaft rings in order from inside to outside, and a linear micro battery with a relatively small diameter was obtained by squeezed to print (Figure 9j, k). Solid and gel polymer electrolytes are considered to be the ultimate choice for future flexible sodium-

metal full batteries with high voltage, high energy density and long cycling life due to their high potential window and good mechanical flexibility. The current challenge for solid electrolytes is to improve ionic conductivity and to address the high impedance caused by interfacial problems. Several recent publications have greatly contributed to the development of flexible sodium ion solid polymer electrolytes.

3.1.4 Flexible Dual-Ion Battery

Sodium-based dual-ion batteries have the advantages of high operating voltage, environmental friendliness, and low cost, but traditional organic electrolytes are easily decomposed at high voltages, resulting in low coulombic efficiency (<60%) of the battery in the discharging/charging process. In addition, the organic electrolyte is also easy to co-intercalate with the graphite electrode to form $C_n^+(solv)_x X^-$ intercalation compound, which causes the graphite-like cathode during

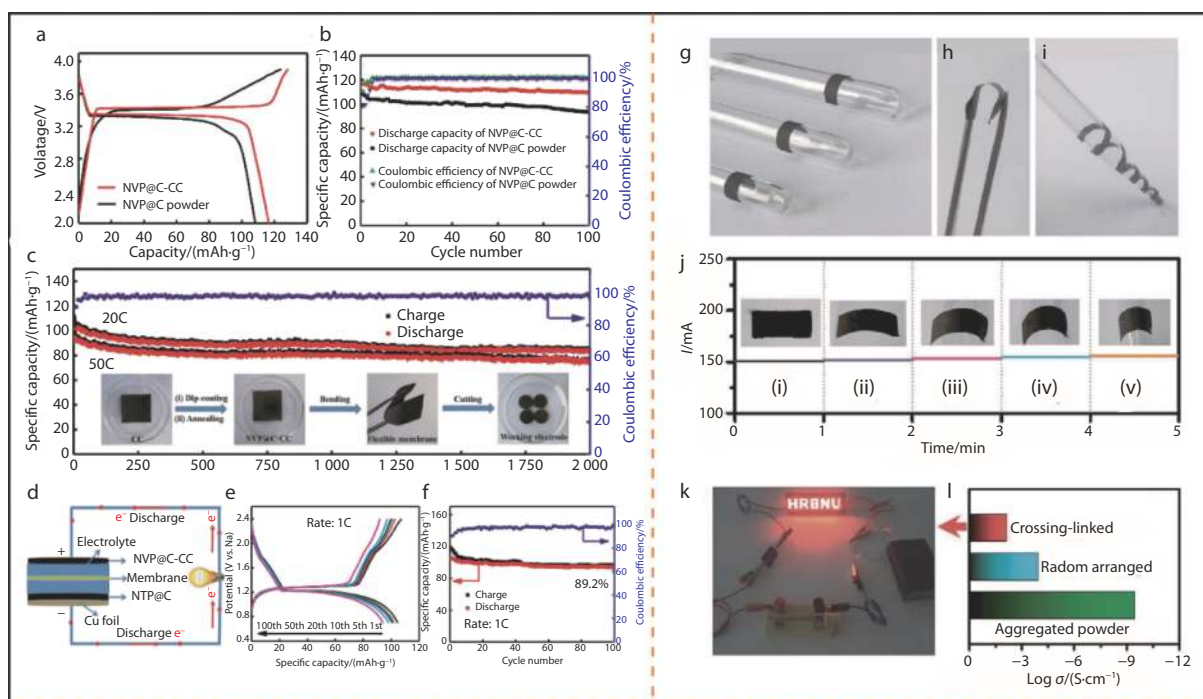


Fig. 8 (a) Voltage profiles of NVP@C-CC and NVP@C powder in the voltage range from 2 to 3.9 V vs. Na^+/Na at 1 C. (b) Cycling performance of NVP@C-CC and NVP@C powder at 1 C. (c) The long-term cycling stability of NVP@C-CC at 20 and 50 C. The inset in (c) is NVP@C-CC film preparation process and flexibility demonstration. (d) Schematic (e) Voltage profiles and (f) Cycling performance of NVP@C-CC/NTP@C full cell in the voltage range from 0.7 to 2.4 V vs. Na^+/Na at 1 C. a-f) Reprinted with permission.^[113] Copyright 2018, Elsevier. (g–i) photographs and (j) current–time curves of the crosslinked nanofiber film bent with different curvatures. In (j), (i) to (v) represent five different bending states. (k) Application of the crosslinked nanofiber as a connection part in an electric circuit. g–k) Reprinted with permission.^[107] Copyright 2019, Royal Society of Chemistry.

the cycling process, thereby exhibiting poor cycling stability. The solid polymer electrolytes are more stable than organic carbonate solvents at high voltages, and the 3D polymer framework of solid electrolytes can alleviate the volume expansion of the electrode. Xie et al.^[117] designed a quasi-solid electrolyte composed of polyvinylidene fluoride-co-hexafluoropropylene (PVDF-HFP) three-dimensionally cross-linked with Al_2O_3 nanoparticles (Figure 10a, b), which has an ion conductivity of up to $1.3 \times 10^{-3} \text{ S cm}^{-1}$, promoting the rapid migration of cations and anions. A all-solid flexible double ion battery was assembled with a graphite cathode and a tin anode in a solid electrolyte as shown in Figure 10c–f. The flexible solid-state double-ion battery has a specific capacity of 96.8 mAh g^{-1} and good cycling stability (97.5% capacity retention after 600 cycles at 5C rate). As shown in Figure 10f, the battery has been folded and squeezed and cycled 60 times with no loss of capacity, indicating a good flexibility. In addition, it can operate over a wide temperature range (-20 to 70°C) (Figure 10g). This high energy density, long cycle stability and excellent high and low temperature solid-state dual ion battery has high potential for flexible energy storage applications.

3.2 Functional application of flexible sodium-ion full battery

In order to better meet the various needs and applications of wearable flexible electronic devices, the design of batteries with various functions and shapes has also aroused researchers' exploration. In recent years, there are reports on

functional flexible sodium-ion batteries, such as stretchable, transparent, self-healing, piezoelectric (flexible batteries that can be charged by external force bending and squeezing). In addition, the shape design of the battery has also evolved from the traditional thick or flat structure to the micro-module integrated system battery to the expandable woven fiber-type battery.

3.2.1 Design of Stretchable Sodium-Ion Battery

For retractable flexible sodium ion batteries, not only the flexibility of the active material but also the ductility of the electrolyte and packaging materials need to be considered^[118]. Gel polymer electrolytes have their own unique advantages in this respect: good stretchable flexibility and freely changed shape and size^[119]. For example, polydimethylsiloxane (PDMS) has high mechanical flexibility and chemical/thermal stability, which can be used as a packaging material for flexible electrodes or an elastic substrate for stretchable devices. So, by matching the flexible electrode material with PDMS gel polymer electrolyte, a flexible sodium ion full battery can be designed. Li et al.^[120] developed a fully-stretched sodium ion full battery with PDMS/rGO sponge/ VOPO_4 as cathode and PDMS/rGO sponge/hard carbon as anode and sodium ion conductive gel polymer as the separator and electrolyte. (Figure 11a–c). The battery exhibited a discharge capacity of $88\text{--}53 \text{ mAh g}^{-1}$ in the current density range of 0.2 to 1 C. After 20% and 50% strain stretching, 96 and 92 mA h g^{-1} can still be maintained. Figure 11d, e demonstrated that the light bulb remained bright after the flexible cell was stretched. This novel design that integrates all stretchable components provides

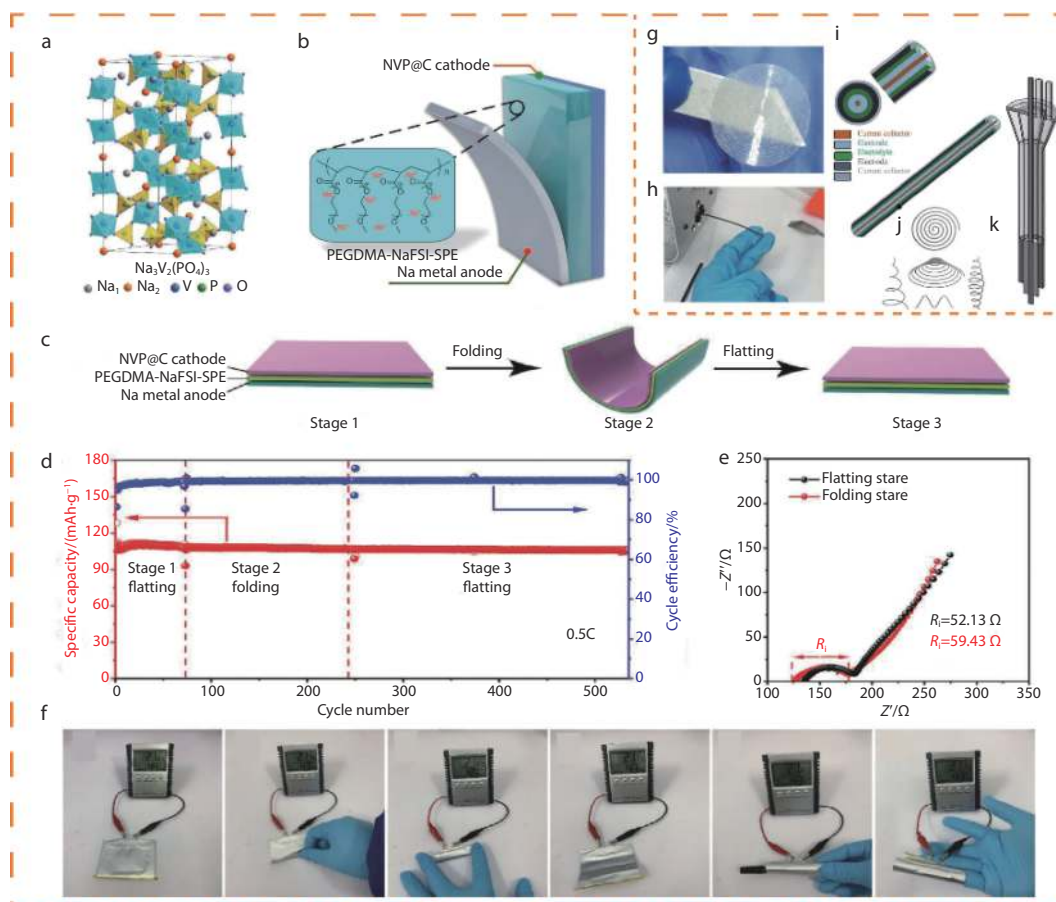


Fig. 9 a) Crystal structure of $\text{Na}_3\text{V}_2(\text{PO}_4)_3$ (NVP). b) The construction architecture of the $\text{NVP@C}|\text{PEGDMA-NaFSI-SPE}|\text{Na}$. c) Schematic of the bendable $\text{NVP@C}|\text{PEGDMA-NaFSI-SPE}|\text{Na}$ ASSB. d) Cycling performance and corresponding Coulombic efficiency at 0.5 C. e) Nyquist plots in flatting or folding state. f) Flexibility and safety evaluation under different conditions of the bendable soft-pack battery. Optical images of the disc-shape printed solid electrolyte. a-f) Reproduced with permission^[115]. Copyright 2018, Wiley-VCH. (g) and cathode filament extrusion (h) and schematic design of multi-coaxial battery (i), possible configurations of printed flexible multi-coaxial cable battery (j), cross-sectional view of the extrusion nozzle (k). g-k) Reproduced with permission^[116]. Copyright 2020, Manchester Nh: Electrical Society.

a way for the next generation of wearable energy devices in modern electronic devices.

3.2.2 Design of self-healing flexible sodium ion battery

Tao et al.^[110] proved that sodium hyaluronate (SH) can be used as a versatile polymer to easily manufacture intrinsically self-healing energy storage devices. According to this principle: the dynamic borate bond can react with the two hydroxyl groups on the SH chain to form a tight cross-linked network (Figure 12a). The author first mixed active materials ($\text{NaTi}_2(\text{PO}_4)_3/\text{C}$ (NTP/C), and $\text{KNi}_{1/3}\text{Fe}_{2/3}(\text{CN})_6$ (KNFC) nanoparticles were used as anode or cathode materials) with a certain amount of borax and SH in deionized water, and then the obtained slurry is cast on a glass mold, and after drying, a cathode film and an anode film were made (Figure 12b). The prepared cathode and anode membranes and SH/ NaNO_3 hydrogel electrolyte can be closely combined to make self-healing sodium ion battery (Figure 12c, d). The self-healing flexible sodium ion battery can maintain a capacity retention rate of 88.3% even after 9 cycles of fracture/healing (Figure 12h, i and j). This design strategy will be likely to promote the development of advanced flexible electronic or intelligent soft robot energy storage equipment^[118].

3.2.3 Design of textileable flexible fiber-based sodium ion battery

For energy storage batteries used in portable wearable electronic devices, it is often necessary to adapt to various complex motion patterns of the human body. Compared with the traditional bagged, cylindrical design flexible battery, the flexible battery designed as a one-dimensional fiber structure has the advantages of being woven and expandable to various devices, and can even be woven directly into a loose woven/knitted piece^[121]. Zhi's group^[122] recently summarized the design principles of fibrous battery, material preparation of different fibrous battery systems, battery assembly, electrochemical performance and flexibility evaluation. In addition, the main technical difficulties faced by the fibrous battery in future wearable applications were discussed, and possible solutions and strategies were proposed for its improvement and development. A few literatures have been reported on flexible fibrous sodium-ion batteries^[55,108,123]. For example, Zhu et al.^[111] recovered electroless nickel plating wastewater and CT waste, and synthesized a flexible electrode substrate NCT with high mechanical strength/flexibility, good electrical conductivity, and good electrochemical stability. Next, the Prussian blue and graphene oxide composite PB@GO was

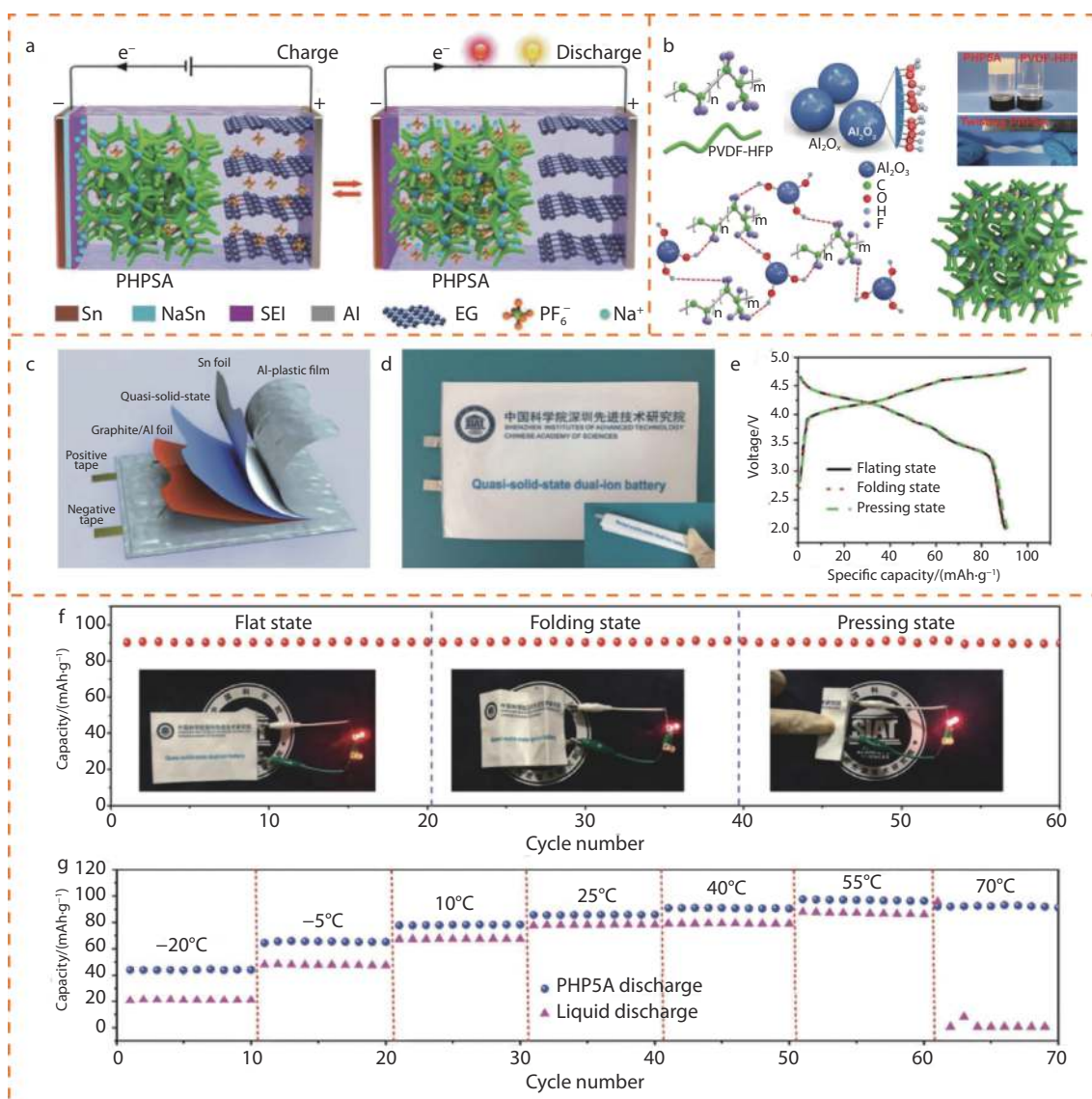


Fig. 10 a) Schematic illustration of the configuration and working mechanism of a QSS-SDIB wherein Na^+ cations migrate to Sn foil anode to form NaSn alloy and PF_6^- anions intercalate into graphite cathode during the charging process. b): i) 3D diagram of PVDF-HFP chemical structure. ii) 3D diagram of Al_2O_3 nanoparticles with hydroxyl on the surface. iii) Typical images of the quasi-solid-state PHPSA after the addition of Al_2O_3 and the liquid state of PVDF-HFP without Al_2O_3 . iv) Typical image of the quasi-solid-state electrolyte under severely twisting. v) Schematic diagram and vi) 3D schematic diagram of the quasi-solid-state polymer PHPA formed by Lewis acid-base intermolecular bonding between PVDF-HFP and Al_2O_3 nanoparticles. c) Schematic structure of the flexible QSS-SDIB. d) Optical photographs of the fabricated flexible QSS-SDIB and the inset is flexible QSS-SDIB in pressed state. e) Charge/discharge profile of flexible QSS-SDIB at the flat, folding, and pressing states. f) Cycling stability of flexible PHPSA-DIB and the insets are the optical photographs of the flexible DIBs under flat, folding, and pressing states, which can light up two LEDs (yellow and red) in series. g) Discharge capacities of the SDIBs based on PHPSA QSE and liquid electrolyte at various temperatures. Reproduced with permission^[117]. Copyright 2018, Wiley-VCH.

loaded on the NCT to obtain a binder-free PB@GO@NCT electrode. More importantly, a new type of tubular flexible wear-resistant SIB was successfully prepared, with good flexibility, high energy density and long cycle life (Figure 13h-l). In addition, in order to determine whether the mechanical stress will reduce the electrochemical performance of the tubular flexible SIB, the discharge performance before and after bending (bending to 30, 60 and 90; bending hundreds of times) was compared; the discharge capacity of one hundred times remained unchanged, indicating that the tubular flexible SIB has high mechanical stability (Figure 13m, n). This strategy

not only opens up a new method for the treatment and reuse of industrial wastewater and waste for new value-added applications, but also has broad application prospects as a flexible wearable device. There are still many problems to be solved in the future application of fibrous batteries in woven wearable devices such as high internal resistance, the installation of the separator, difficulty in packaging, the large diameter of the battery, large-scale manufacturing issues.

3.2.4 Piezoelectric self-charging flexible sodium ion battery

In recent years, piezoelectric nanogenerators (PENGs) can be easily collected and convert surrounding mechanical en-

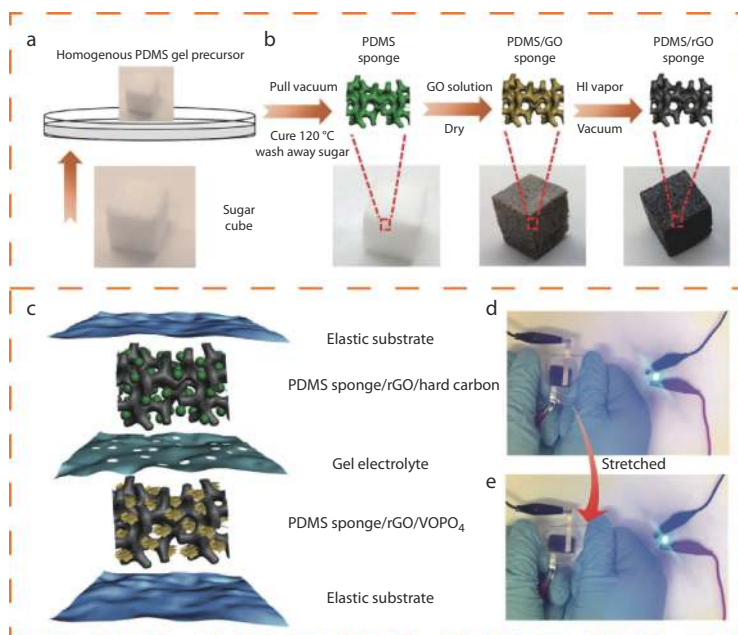


Fig. 11 Schematic of preparation steps of conductive PDMS/rGO sponge. a) While the PDMS/GO sponge (insulating) was brownish in color, once the material was reduced to rGO (conductive), the material appeared black. Schematic of preparation steps of conductive PDMS/rGO sponge. b) While the PDMS/GO sponge (insulating) was brownish in color, once the material was reduced to rGO (conductive), the material appeared black. c) Schematic illustration of the fabricated stretchable PDMS/rGO sponge/VOPO₄//PDMS/rGO sponge/hard carbon sodium-ion full battery. d,e) Photographs of the stretchable sodium-ion full battery in the unstretched state (top) and stretched state with ≈50% strains (bottom) to power a commercial LED light. a-e) Reproduced with permission^[120]. Copyright 2017, Wiley-VCH.

ergy into electrical energy due to the piezoelectric effect, which has attracted increasing attention^[126]. Combining the working characteristics of flexible batteries that are often bent and squeezed with the advantages of PENGs that spontaneously collect mechanical energy to convert it into electrical energy, they can be freed from frequent charging outside the battery and become self-sufficient. Zhou et al.^[125] prepared porous elastic KNN-SEBS piezoelectric-separators coupling piezoelectric by mixing potassium sodium niobate (KNN) piezoelectric particles with styrene-ethylene-butene-styrene (SEBS) polymer, which were then deposited on the surface of glass fiber membrane. A flexible rechargeable sodium ion full battery (SCSIB) was assembled with the Na₃V₂(PO₄)₃(NVP)/C as cathode and Ni₂P@PNC as anode material. Figure 14a shows the structure of a flexible SCSIB, that the glass fiber membrane is layered with KNN@SEBS flexible porous piezoelectric membrane on the surface to form the combined separator of the battery, which differs from the structure of a common sodium ion battery. The synthesis process of the KNN@SEBS porous elastic piezoelectric film, which was the core component of the flexible SCSIB, was shown in Figure 14c. As shown in Figure 14b, the flexible SCSIB can be wound into a circle. In addition, it can be bent to different angles (0, 45 and 90°) (iii-v). As shown in the Figure 15f-i, the battery can be randomly bent for 150 seconds or can stand 300-second hand tap to charge to about 0.65 V. Interestingly, a considerable self-charging response can be obtained even at static voltage. Figure 14j demonstrates that by connecting four flexible SCSIBs in series, a simple tap is able to raise the voltage to 1.43 V–2.10 V in 300 s. Theoretically, the piezoelectric effect is closely related to the generation of electric dipoles under strain/deformation^[127,134]. The cathode and

anode charge centers of a piezoelectric material was separated, forming an electric dipole, and thus generating a piezoelectric potential^[127]. This potential can drive the flow of free electrons in an external circuit, thus converting mechanical energy into electrical energy^[127]. Here, the perforated elastic KNN piezoelectric film due to the piezoelectric effect allows the electrochemical equilibrium in the device to be disrupted by external forces and the migration of Na from the cathode to the anode. At the same time, an electrochemical reaction takes place (cathode: Na₃V₂(PO₄)₃ → NaV₂(PO₄)₃ + 2Na⁺ + 2e⁻; anode: Ni₂P + 3Na⁺ + 3e⁻ → Na₃P + 2Ni, Na₃P → P + 3Na⁺ + 3e⁻) (Figure 14d). From the outside, due to the high elasticity of the piezoelectric film, it has an excellent energy absorption capacity and retains a large residual stress inside even when the external force is removed, maintaining the force to electricity conversion process. As a result, the electrochemical reaction continues to generate a piezoelectric potential (Figure 14i). In addition, even under static pressure, a considerable self-charging response can be obtained, which further promotes its application in flexible energy storage devices in multi-frequency bending and extrusion scenarios, such as the design of a flexible self-recharging insole battery. The power for walking can be converted into electrical energy and stored (Figure 14e).

To date, state-of-the-art PENGs are generally made of piezoelectric materials whose flexibility and extensibility facilitate the integration of various energy storage units or wearable electronics. This integration of piezoelectric materials separator benefit for self-rechargeable hybrid designs and avoid the dependence on frequent charging of batteries via external chargers, in which the mechanical energy can be converted into electrical energy via piezoelectricity^[128–133]. In

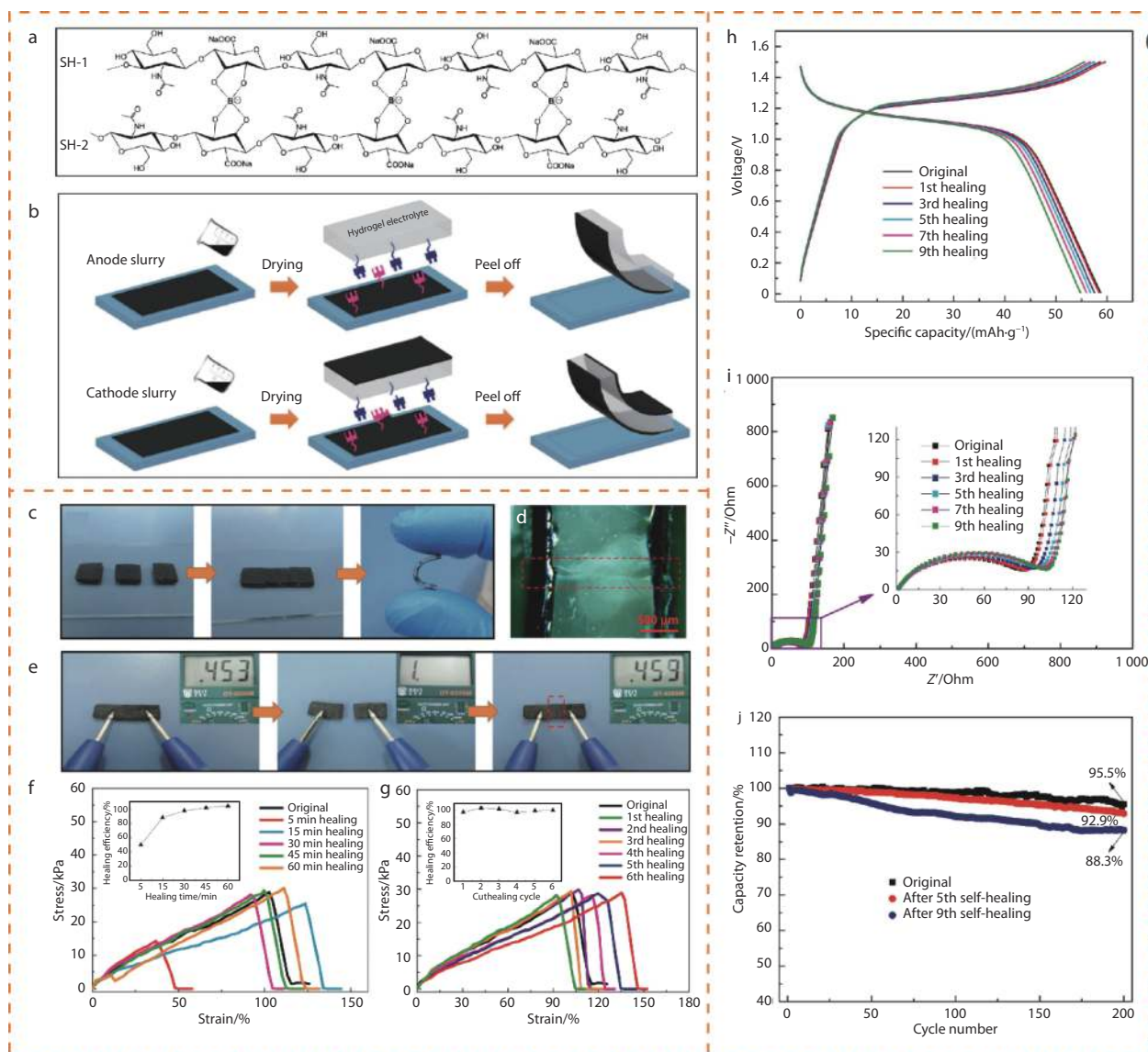


Fig. 12 Illustration of the (a) formation of dynamic borate ester bonding between SH chains and (b) fabrication of a self-healable SIB or asymmetric capacitor. The anode and cathode films are first prepared through a casting process and then successively coated onto the opposite sides of the SH/NaNO₃ hydrogel electrolyte. (c) Self-healing of the SIB after cutoff under ambient conditions. (d) Cross-sectional image of the healed region observed by optical microscopy. (e) Resistance variation of the battery during the cut/healing process. Stress-strain curves of the battery (f) at different healing stages and (g) after multiple cut/healing cycles. The insets are the mechanical healing efficiency calculated from the corresponding stress-strain curves. The healing duration for each cycle was 60 min. Electrochemical performances of the SIB and the asymmetric capacitor before and after self-healing. GCD profiles of the (h) battery at 0.2 A g⁻¹ and (i) Nyquist plots of the battery. Cycling characteristics of the (j) battery at 0.2 A g⁻¹. Reproduced with permission.^[110] Copyright 2019, American Chemical Society.

addition, this design helps to eliminate unnecessary charging circuits and external electrical connections. The reduced size, structure and weight facilitates wearable electronics applications^[134]. To date, state-of-the-art PENGs are generally made of piezoelectric materials whose flexibility and extensibility facilitate the integration of various energy storage units or wearable electronics. This integration of piezoelectric materials separator benefit for self-rechargeable hybrid designs and avoid the dependence on frequent charging of batteries *via* external chargers, in which the mechanical energy can be converted into electrical energy *via* piezoelectricity^[128–133]. In addition, this design helps to eliminate unnecessary charging circuits and external electrical connections. The reduced size,

structure and weight facilitates wearable electronics applications^[134].

4 Summary and outlook

Since current research on flexible sodium ion batteries has been focused on the preparation of various flexible cell materials, but there are still very few truly flexible sodium ion batteries, and the testing and evaluation of flexible electrode materials and devices for flexible sodium ion batteries are not well developed. Here, we review the relevant methods for evaluating device flexibility. In addition, we describe the challenges and prospects of flexible sodium ion batteries in terms

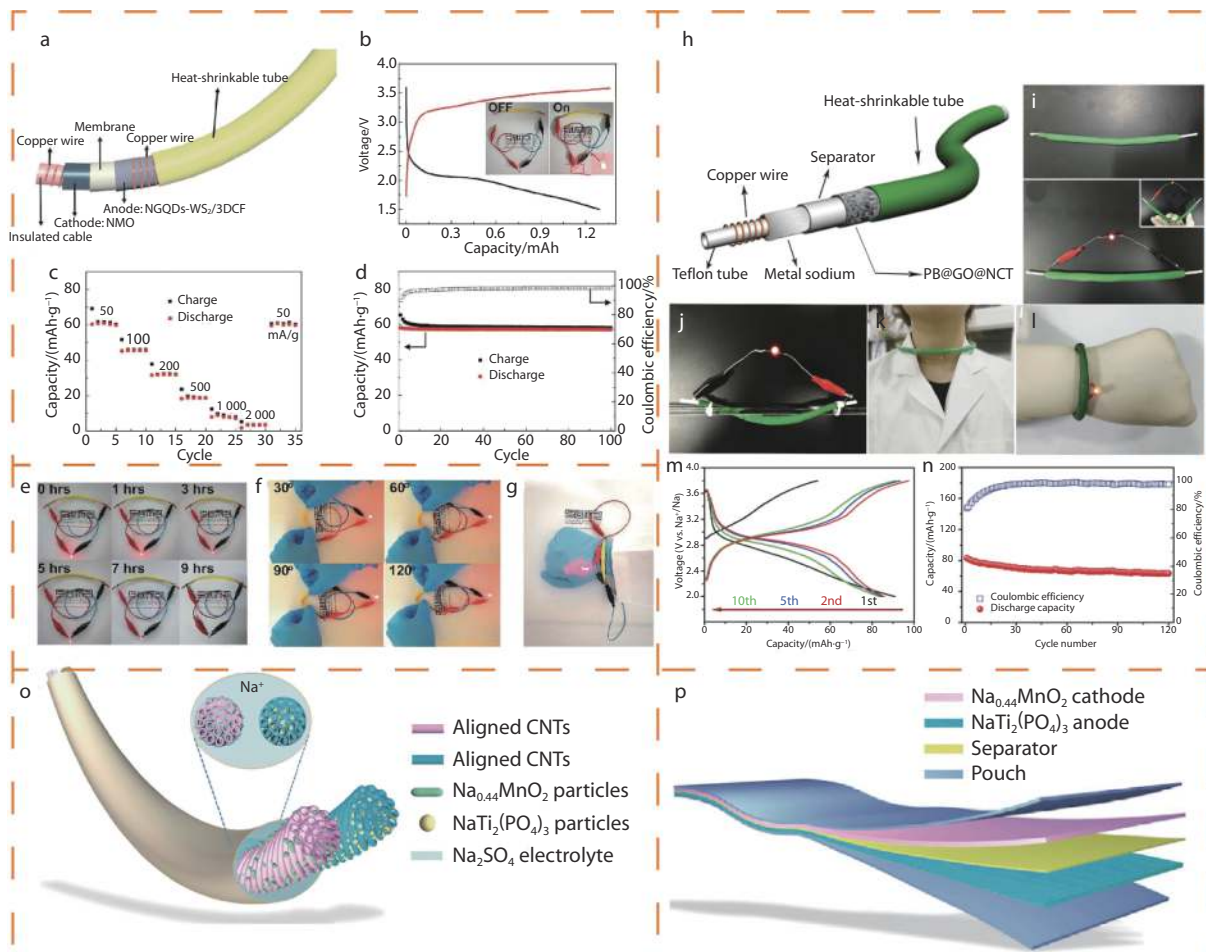


Fig. 13 Flexible cable-shaped SIB with NGQDs-WS₂/3DCF as the anode electrode. (a) Schematic of the structure. (b) Galvanostatic charge and discharge curves at a current of 3 mA (third cycle after two pre-activation cycles). The inset is the cable-shaped SIB to power a red LED with off and on status. (c) Rate capability and (d) cycle stability and related coulombic efficiency at a current density of 50 mA g⁻¹ of the cable-shaped SIBs. (e) A red LED powered by a 7 cm cable-shaped SIB for 9 hours. (f) Photographs of a red LED powered by the cable-shaped SIB at various bending angles. (g) Picture of the cable-shaped SIB as a wrist strap battery to power a red LED. a-g) Reproduced with permission^[108]. Copyright 2018, Royal Society of Chemistry. h) Schematic illustration for the structure of the tube-type flexible SIBs. i) Digital photograph of the fabricated tube-type flexible SIBs. j-l) Demonstration of an LED lighting by tube-type flexible SIBs under different conditions. m) Charge-discharge profiles of tube-type flexible SIBs at a current density of 50 mA g⁻¹. n) Cycles performance of tube-type flexible SIBs at a current density of 100 mA g⁻¹. h-n) Reproduced with permission^[111]. Copyright 2017, Wiley-VCH. o) the Flexible Belt-Shaped and p) Flexible Fiber-Shaped Na_{0.44}MnO₂//NaTi₂(PO₄)₃@C Battery Using 1 M Na₂SO₄ as Electrolyte. o, p) Reproduced with permission^[124]. Copyright 2017, Elsevier.

of cell lifetime, energy and power density, flexibility and biocompatibility, safety, and multifunctional integration. Finally, we provide insight into how the basic components of flexible sodium-ion batteries (electrodes, electrolytes, separator, and packaging materials) can be matched to meet different market needs, and list several new flexible sodium-ion batteries with great commercialization potential from an application perspective. Figure 15 compares the performance of current common cathode, anode, electrolytes, and flexible substrates based on specific capacity, voltage, rate, Initial coulombic efficiency, cost, potential window, environmental friendliness, safety, cycling stability, flexibility, mechanical properties, and loading capacity. The most commercially promising cathode materials are layered oxides, Prussian blue analogs, and polyanionic materials. Among them, dehydrated Prussian blue is considered the most promising cathode material for commercialization due to its high specific ca-

capacity, excellent rate performance and abundant resources (Figure 15a). However, in the field of flexible sodium ion batteries, in addition to the active material, some substrates that act as support and flexibility are also critical. Sometimes to optimize mechanical flexibility, the high quality share of inactive material substrates largely sacrifices the energy density material of the device. In addition the common carbon nanofibers, carbon cloth, carbon nanotubes and graphene substrates are much more expensive than aluminum foil (Figure 15c, d). Thus for flexible sodium ion batteries, inexpensive Dehydrated PB cathode materials have little advantage to offer until the issue of cycling stability is addressed. For commercialized non-flexible sodium ion battery cathode materials, non-graphitized carbon will greatly improve the specific energy density matched with cathode materials because of its higher Initial Coulombic efficiency, low voltage plateau and higher reversible capacity. Therefore, based on the conven-

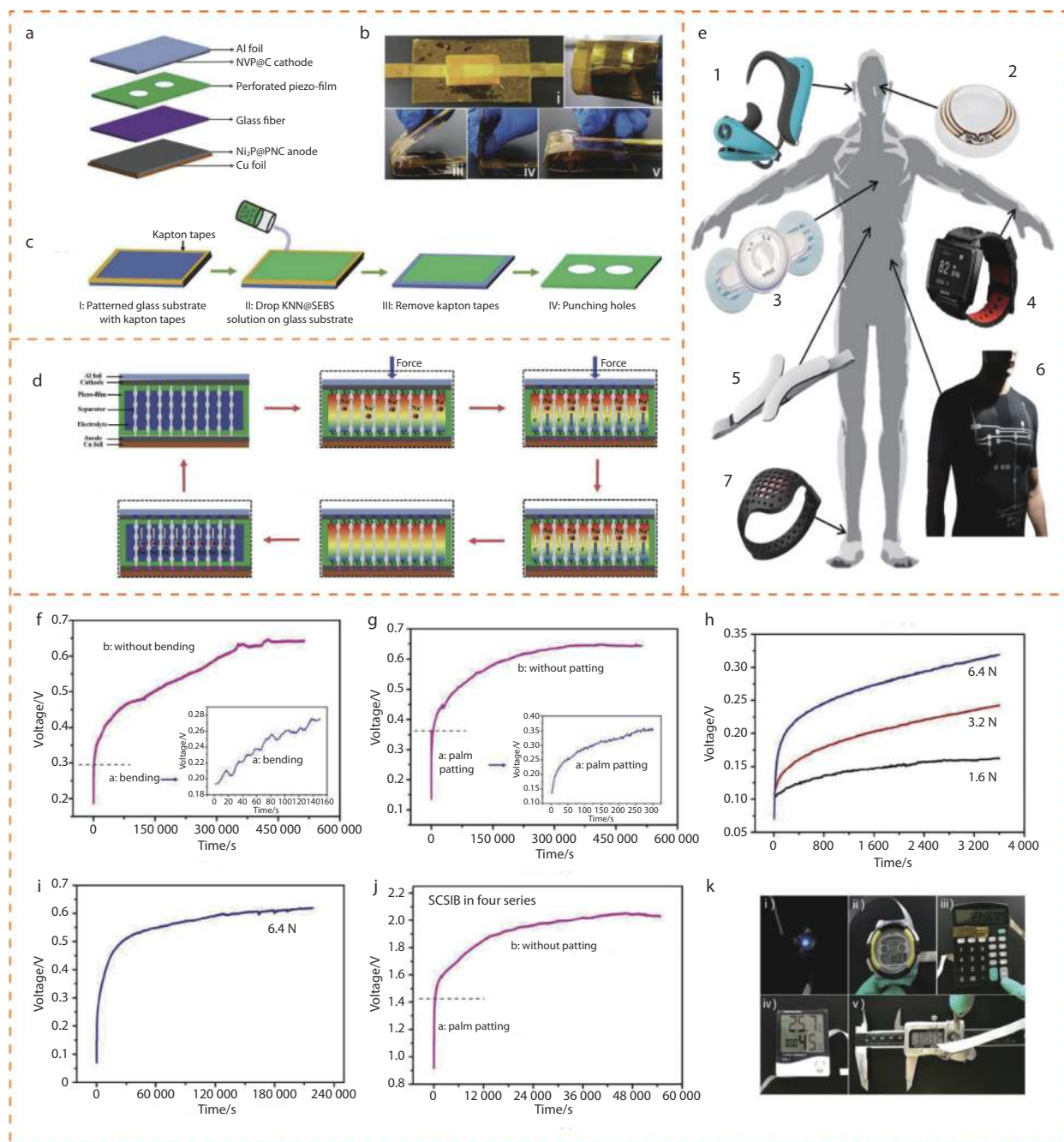


Fig. 14 (a) Device architecture of the flexible SCSIB. (b) SCSIB demonstrates excellent flexibility: i) optical image of a flexible SCSIB, ii) SCSIB can be rolled in a circle, iii-v) SCSIB can be bent with various angles (0°, 45°, and 90°), (c) Synthetic procedure of the perforated elastic KNN@SEBS piezo-film for the flexible SCSIB, (d) Schematic illustration of the self-charging mechanism of the flexible SCSIB. (e) Various wearable devices based on the human body in the future. Self-charging behaviors of the flexible SCSIB: (f) Self-charging process of a single device treated by bending (the inset is the enlarged charging curve at the initial 300 s), (g) Self-charging process of a single device treated by palm patting (the inset is the enlarged charging curve at the initial 300 s), (h) Self-charging curve of a single device treated by loading at 1.6, 3.2 and 6.4 N in 3600 s, (i) Self-charging curve of a single device applied at 6.4 N with long-time, (j) Self-charging curve of four serially connected flexible devices treated by palm patting and (k) some display applications (i-iv): the serially connected devices can power a LED light, a smartwatch, an electric calculator, a humidity indicator, and a digital Vernier caliper. a-d, f-k) Reproduced with permission^[125]. Copyright 2019, Elsevier.

tionalorganic-basedall-cellPB@substrate//HC/NVP@substrate//HC@substrate; NaMxMy'M"zO₂@substrate//HC@substrate matching seems to be the most excellent choice. However, in flexible batteries, considering the long-term mechanical deformation conditions, aqueous electrolytes will play a role in

the field of flexible sodium ion batteries due to their lower cost and non-toxic characteristics based on the inevitable risk of permeation of conventional organic-based electrolytes. The symmetry-based NASION full cell has a great advantage in high power applications due to its large multiplier perform-

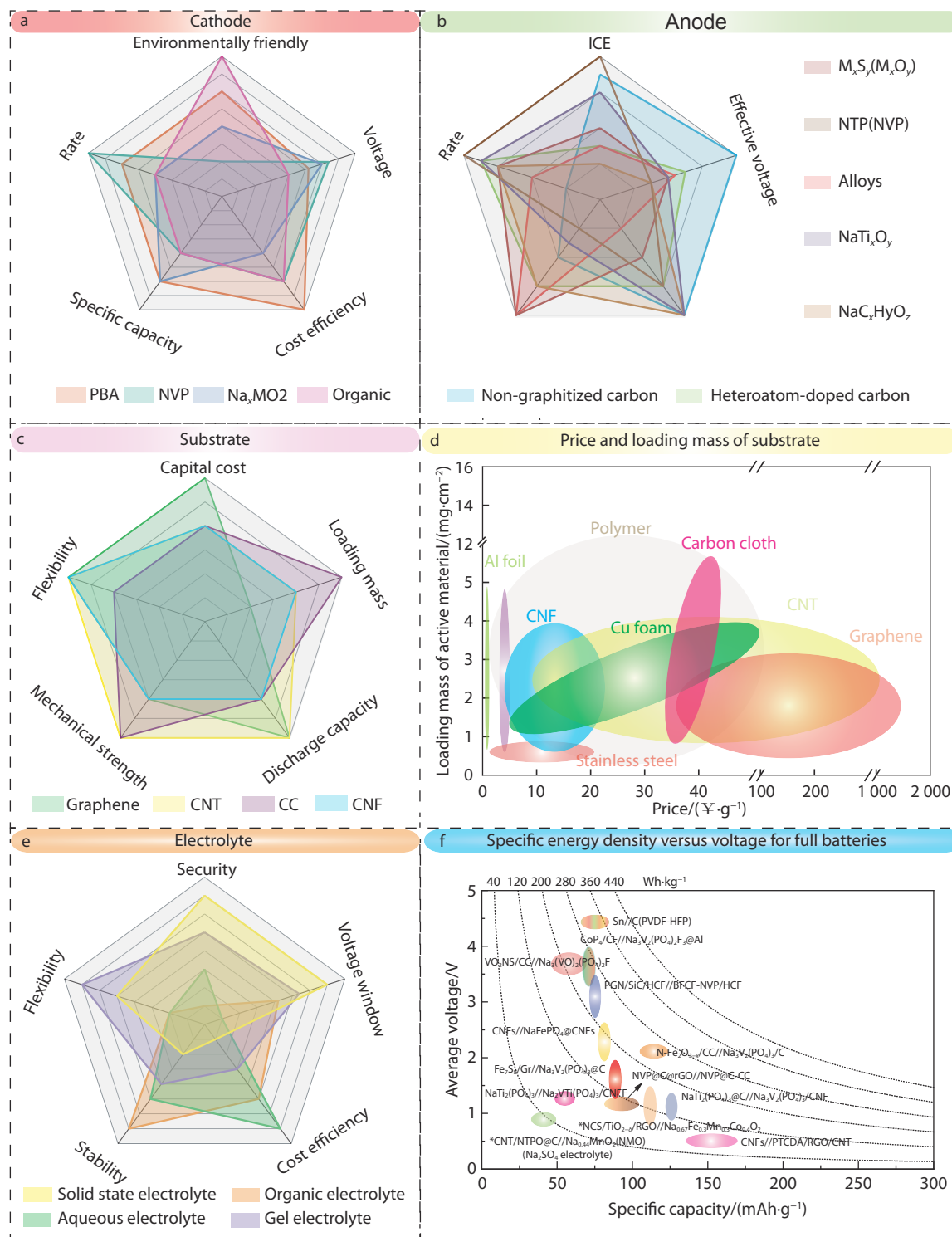


Fig. 15 Comparison of various performance indicators of a) Cathode; b) Anode; c) Substrate; e) Electrolyte. d) Comparison of loading mass and price for different substrates. f) Comparison of full cell specific energy density with different cathode and anode material matching.

ance. It has a low potential window just sign to be compatible with aqueous electrolytes, which is ideal for wearable applications with high safety requirements. As shown in Figure 15e, f, flexible solid state sodium ion batteries and flexible dual ion batteries have high energy density due to their high potential window, however both have many difficult funda-

mental problems such as low ionic conductivity of solid state electrolytes and poor interface issues. Dual ion batteries also require an electrolyte with high potential or a solid state electrolyte to work.

Flexible sodium ion batteries capable of standing demanding deformation conditions, such as stretching, twisting, or

even cropping, will further increase the scope of future applications, such as stretchable sodium ion batteries or self-healing sodium ion batteries. Such complex shaped batteries may also require the use of gel electrolytes to match. Stretchable or self-healing batteries can be prepared by integrating the cathode material, the gel electrolyte and the anode material. The deformation conditions can also be improved to some extent by improvements in the physical structure construction. For example, the design of micro-fiber type batteries, by integrating the textile as wearable batteries. In addition, the integration of other physical or biological functions into flexible sodium ion batteries is also attracting increasing attention, such as the design of self-charging flexible sodium ion batteries by combining the mechanical deformation of piezoelectric nanogenerators (PENGs) with the bendable characteristics of flexible sodium ion batteries. This direct conversion of mechanical energy into electrical energy can greatly reduce the loss of resources and achieve self-sufficiency to a certain extent.

Acknowledgments

This work was financially supported by the National Natural Science Foundation of China (No. 51971124).

Conflict of interest

The authors declare no conflict of interest.

Author contributions

Xiangxi He: Survey, data compilation, writing-original draft. Jiahua Zhao: Data collation. Weihong Lai: Overview outline revision. Zhuo Yang: Writing-Review & Editing. Yun Gao: Writing Review & Editing. Hang Zhang: Writing-Review & Editing. Li-Li: Supervision, Writing-Review & Editing. Shu-Lei Chou: Writing Review & Editing, Funding acquisition.

REFERENCES

1. a) L. Li, Z. Wu, S. Yuan, X.-b. Zhang, *Energy Environ. Sci.* 2014, 7, 2101.; b) S.-Y. Lee, K.-H. Choi, W.-S. Choi, Y. H. Kwon, H.-R. Jung, H.-C. Shin, J. Y. Kim, *Energy Environ. Sci.* 2013, 6, 2414
2. X. Wang, X. Lu, B. Liu, Di Chen, Y. Tong, G. Shen, *Adv. Mater.*, 2014, 26, 4763
3. a) G. Zhou, F. Li, H.-M. Cheng, *Energy Environ. Sci.* 2014, 7, 1307.; b) H. Gwon, J. Hong, H. Kim, D.-H. Seo, S. Jeon, K. Kang, *Energy Environ. Sci.* 2014, 7, 538; c) L. Wang, Di Chen, K. Jiang, G. Shen, *Chemical Society Reviews* 2017, 46, 6764
4. a) Z. Yang, X. Liu, X. He, W. Lai, L. Li, Y. Qiao, S. Chou, M. Wu, *Adv. Funct. Mater.* 2020, 31, 2006457.; b) Y. Gao, H. Zhang, X. Liu, Z. Yang, X. He, L. Li, Y. Qiao, S. Chou, *Adv. Ener. Mater.* 2021, 11, 2101751
5. A. Sumboja, J. Liu, W. G. Zheng, Y. Zong, H. Zhang, Z. Liu, *Chemical Society Reviews*, 2018, 47, 5919
6. H. Li, X. Zhang, Z. Zhao, Z. Hu, X. Liu, G. Yu, *Energy Storage Mater.*, 2020, 26, 83
7. T. Jin, Q. Q. Han, L. F. Jiao, *Adv. Mater.*, 2020, 32, 1806304
8. M. Chen, D. Cortie, Z. Hu, H. Jin, S. Wang, Q. Gu, W. Hua, E. Wang, W. Lai, L. Chen, et al, *Adv. Energy Mater.*, 2018, 8, 1800944
9. H. Shi, G. Wen, Y. Nie, G. Zhang, H. Duan, *Nanoscale*, 2020, 12, 5261
10. C. Wu, X. H. Zeng, P. G. He, L. B. Chen, W. F. Wei, *Advanced Materials Interfaces*, 2018, 5, 1701080
11. Y. Yao, M. L. Chen, R. Xu, S. F. Zeng, H. Yang, S. F. Ye, F. F. Liu, X. J. Wu, Y. Yu, *Adv. Mater.*, 2018, 30, 1805234
12. D. Z. Kong, Y. Wang, Y. von Lim, S. Z. Huang, J. Zhang, B. Liu, T. P. Chen, H. Y. Yang, *Nano Energy*, 2018, 49, 460
13. H. Zhang, Y. Gao, X.-H. Liu, Z. Yang, X.-X. He, L. Li, Y. Qiao, W.-H. Chen, R.-H. Zeng, Y. Wang, et al, *Adv. Funct. Mater.*, 2021, 32, 2107718
14. H. Li, Z. Tang, Z. Liu, C. Zhi, *Joule*, 2019, 3, 613
15. J. Chang, Q. Huang, Y. Gao, Z. Zheng, *Adv. Mater.*, 2021, 33, 2004419
16. C. Zhao, Y. Lu, L. Chen, Y.-S. Hu, *InfoMat*, 2020, 2, 126
17. X.-X. He, X.-H. Liu, Z. Yang, H. Zhang, L. Li, G. Xu, Y. Qiao, S.-L. Chou, M. Wu, *Electrochemistry Communications*, 2021, 128, 107067
18. S. N. Liu, Z. G. Luo, G. Y. Tian, M. N. Zhu, Z. Y. Cai, A. Q. Pan, S. Q. Liang, *J. Power Sources*, 2017, 363, 284
19. Z. H. Li, W. Shen, C. Wang, Q. J. Xu, H. M. Liu, Y. G. Wang, Y. Y. Xia, *J. Mater. Chem. A*, 2016, 4, 17111
20. K. Wang, Y. Huang, M. Y. Wang, M. Yu, Y. D. Zhu, J. S. Wu, *Carbon*, 2017, 125, 375
21. C. S. Zhou, S. X. Fan, M. X. Hu, J. M. Lu, J. Li, Z. H. Huang, F. Y. Kang, R. T. Lv, *J. Mater. Chem. A*, 2017, 5, 15517
22. S. A. Liu, Z. Y. Cai, J. Zhou, M. N. Zhu, A. Q. Pan, S. Q. Liang, *J. Mater. Chem. A*, 2017, 5, 9169
23. Z. H. Zhao, X. D. Hu, H. Q. Wang, M. Y. Ye, Z. Y. Sang, H. M. Ji, X. L. Li, Y. J. Dai, *Nano Energy*, 2018, 48, 526
24. X.-X. He, J.-H. Zhao, W.-H. Lai, R. Li, Z. Yang, C.-m. Xu, Y. Dai, Y. Gao, X.-H. Liu, L. Li, et al, *ACS Appl. Mater. Interfaces*, 2021, 13, 44358
25. H. Zhu, C. Y. Wang, C. Y. Li, L. L. Guan, H. G. Pan, M. Yan, Y. Z. Jiang, *Carbon*, 2018, 130, 145
26. X. Z. Sun, C. L. Wang, Y. Gong, L. Gu, Q. W. Chen, Y. Yu, *Small*, 2018, 14, 1802218
27. X. J. Wang, K. Z. Cao, Y. J. Wang, L. F. Jiao, *Small*, 2017, 13(29), 1700623
28. T. Liu, K. C. Kim, B. Lee, Z. Chen, S. Noda, S. S. Jang, S. W. Lee, *Energy Environ. Sci.*, 2017, 10, 205
29. X. W. Wang, H. P. Guo, J. Liang, J. F. Zhang, B. Zhang, J. Z. Wang, W. B. Luo, H. K. Liu, S. X. Dou, *Adv. Funct. Mater.*, 2018, 28, 1801016
30. M. H. Chen, D. L. Chao, J. L. Liu, J. X. Yan, B. W. Zhang, Y. Z. Huang, J. Y. Lin, Z. X. Shen, *Adv. Funct. Mater.*, 2017, 27, 1606232
31. J. T. Xu, M. Wang, N. P. Wickramaratne, M. Jaroniec, S. X. Dou, L. M. Dai, *Adv. Mater.*, 2015, 27(12), 2042–2048
32. Y. H. Liu, A. Y. Zhang, C. F. Shen, Q. Z. Liu, X. A. Cao, Y. Q. Ma, L. A. Chen, C. Lau, T. C. Chen, F. Wei, et al, *ACS Nano*, 2017, 11, 5530
33. N. Sun, Y. Guan, Y.-T. Liu, Q. Zhu, J. Shen, H. Liu, S. Zhou, B. Xu, *Carbon*, 2018, 137, 475
34. Y. Liu, Y. Z. Yang, X. Z. Wang, Y. F. Dong, Y. C. Tang, Z. F. Yu, Z. B. Zhao, J. S. Qiu, *ACS Appl. Mater. Interfaces*, 2017, 9, 15484
35. T. Y. Liu, B. Lee, B. G. Kim, M. J. Lee, J. Park, S. W. Lee, *Small*, 2018, 14, 1801236
36. J. J. He, N. Wang, Z. L. Cui, H. P. Du, L. Fu, C. S. Huang, Z. Yang, X. Y. Shen, Y. P. Yi, Z. Y. Tu, et al, *Nat Commun*, 2017, 8, 1
37. H. Bian, J. Zhang, M.-F. Yuen, W. Kang, Y. Zhan, D. Y. W. Yu, Z. Xu, Y. Y. Li, *J. Power Sources*, 2016, 307, 634
38. H. Wang, X. Gao, J. Feng, S. Xiong, *Electrochim. Acta*, 2015, 182, 769
39. H.-Y. Lu, X.-H. Zhang, F. Wan, D.-S. Liu, C.-Y. Fan, H.-M. Xu, G. Wang, X.-L. Wu, *ACS Appl. Mater. Interfaces*, 2017, 9, 12518
40. J. Fei, Y. L. Cui, J. Y. Li, Z. W. Xu, J. Yang, R. Y. Wang, Y. Y. Cheng, J. F. Hang, *Chemical Communications*, 2017, 53, 13165
41. H. Y. Wang, H. Jiang, Y. J. Hu, P. Saha, Q. L. Cheng, C. Z. Li, *Chem-*

- ical Engineering Science*, 2017, 174, 104
42. W. N. Ren, H. F. Zhang, C. Guan, C. W. Cheng, *Adv. Funct. Mater.*, 2017, 27, 1702116
 43. Y. Zhang, Z. Q. Liu, H. Y. Zhao, Y. P. Du, *Rsc Advances*, 2016, 6, 1440
 44. X. Wei, W. H. Li, J. A. Shi, L. Gu, Y. Yu, *ACS Appl. Mater. Interfaces*, 2015, 7, 27804
 45. Y. Wang, C. Wu, Z. Wu, G. Cui, F. Xie, X. Guo, X. Sun, *Chemical Communications*, 2018, 54, 9341
 46. M. S. Balogun, Y. Luo, F. Y. Lyu, F. X. Wang, H. Yang, H. B. Li, C. L. Liang, M. Huang, Y. C. Huang, Y. X. Tong, *ACS Appl. Mater. Interfaces*, 2016, 8, 9733
 47. P. Nie, L. F. Shen, G. Pang, Y. Y. Zhu, G. Y. Xu, Y. H. Qing, H. Dou, X. G. Zhang, *J. Mater. Chem. A*, 2015, 3, 16590
 48. Y. Bao, Y. P. Huang, X. Song, J. Long, S. Q. Wang, L. X. Ding, H. H. Wang, *Electrochim. Acta*, 2018, 276, 304
 49. H. Tao, L. Xiong, S. Du, Y. Zhang, X. Yang, L. Zhang, *Carbon*, 2017, 122, 54
 50. X. J. Wang, Y. C. Liu, Y. J. Wang, L. F. Jiao, *Small*, 2016, 12, 4865
 51. S. Gao, G. Chen, Y. Dall'Agnese, Y. J. Wei, Z. M. Gao, Y. Gao, *Chemistry-a European Journal*, 2018, 24, 13535
 52. G. S. Chen, X. Yao, Q. C. Cao, S. X. Ding, J. D. He, S. Q. Wang, *Materials Letters*, 2019, 234, 121
 53. Y. L. Pan, X. D. Cheng, Y. J. Huang, L. L. Gong, H. P. Zhang, *ACS Appl. Mater. Interfaces*, 2017, 9, 35820
 54. H. Yin, H.-Q. Qu, Z. Liu, R.-Z. Jiang, C. Li, M.-Q. Zhu, *Nano Energy*, 2019, 58, 715
 55. Q. Chen, S. Sun, T. Zhai, M. Yang, X. Y. Zhao, H. Xia, *Adv. Energy Mater.*, 2018, 8, 1800054
 56. X. Q. Xiong, W. Luo, X. L. Hu, C. J. Chen, L. Qie, D. F. Hou, Y. H. Huang, *Scientific Reports*, 2015, 5, 9254
 57. H. Yang, M. Wang, X. W. Liu, Y. Jiang, Y. Yu, *Nano Research*, 2018, 11, 3844
 58. W. Li, R. Bi, G. X. Liu, Y. X. Tian, L. Zhang, *ACS Appl. Mater. Interfaces*, 2018, 10, 26982
 59. C. T. Zhao, C. Yu, M. D. Zhang, Q. Sun, S. F. Li, M. N. Banis, X. T. Han, Q. Dong, J. Yang, G. Wang, et al, *Nano Energy*, 2017, 41, 66
 60. M. L. Mao, C. Y. Cui, M. G. Wu, M. Zhang, T. Gao, X. L. Fan, J. Chen, T. H. Wang, J. M. Ma, C. S. Wang, *Nano Energy*, 2018, 45, 346
 61. M. Zhu, Z. Luo, A. Pan, H. Yang, T. Zhu, S. Liang, G. Cao, *Chem. Eng. J.*, 2018, 334, 2190
 62. L. L. Luo, B. Cheng, S. J. Chen, Z. C. Ge, H. T. Zhuo, *Materials Letters*, 2018, 232, 153
 63. C. Deng, S. Zhang, H. Wang, G. Zhang, *Nano Energy*, 2018, 49, 419
 64. T. T. Yu, B. Lin, Q. F. Li, X. H. Wang, W. L. Qu, S. Zhang, C. Deng, *Physical Chemistry Chemical Physics*, 2016, 18, 26933
 65. X. Zhang, J. Zhou, C. Liu, X. Chen, H. Song, *J. Mater. Chem. A*, 2016, 4, 8837
 66. H. R. An, Y. Li, Y. Gao, C. Cao, J. K. Han, Y. Y. Feng, W. Feng, *Carbon*, 2017, 116, 338
 67. N. Q. Tran, T. A. Le, H. Lee, *J. Mater. Chem. A*, 2018, 6, 17495
 68. W. Liu, B. Shi, Y. Wang, Y. Li, H. J. Pei, R. Guo, X. W. Hou, K. Zhu, J. Y. Xie, *Chemistryselect*, 2018, 3, 5608
 69. P. L. Zheng, Z. F. Dai, Y. Zhang, K. N. Dinh, Y. Zheng, H. S. Fan, J. Yang, R. Dangol, B. Li, Y. Zong, et al, *Nanoscale*, 2017, 9, 14820
 70. W. W. Xu, K. N. Zhao, L. Zhang, Z. Q. Xie, Z. Y. Cai, Y. Wang, *Journal of Alloys and Compounds*, 2016, 654, 357
 71. X. X. Ma, L. Chen, X. H. Ren, G. M. Hou, L. N. Chen, L. Zhang, B. B. Liu, Q. Ai, P. C. Si, J. Lou, et al, *J. Mater. Chem. A*, 2018, 6, 1574
 72. Y. H. Liu, A. Y. Zhang, C. F. Shen, Q. Z. Liu, J. S. Cai, X. Cao, C. W. Zhou, *Nano Research*, 2018, 11, 3780
 73. S. Zhang, C. Deng, Y. Meng, *J. Mater. Chem. A*, 2014, 2, 20538
 74. D. Yang, X.-Z. Liao, J. Shen, Y.-S. He, Z.-F. Ma, *Journal of Materials Chemistry A*, 2014, 2, 6723
 75. F. X. Bu, P. T. Xiao, J. D. Chen, M. F. A. Aboud, I. Shakir, Y. X. Xu, *J. Mater. Chem. A*, 2018, 6, 6414
 76. H. Chu, Y. Pei, Z. Cui, C. Steven, P. Dong, P. M. Ajayan, M. X. Ye, J. F. Shen, *Nanoscale*, 2018, 10, 14697
 77. J. Y. Xiang, D. D. Dong, F. S. Wen, J. Zhao, X. Y. Zhang, L. M. Wang, Z. Y. Liu, *Journal of Alloys and Compounds*, 2016, 660, 11
 78. D. L. Chao, C. R. Zhu, X. H. Xia, J. L. Liu, X. Zhang, J. Wang, P. Liang, J. Y. Lin, H. Zhang, Z. X. Shen, et al, *Nano Lett.*, 2015, 15, 565
 79. T. C. Yuan, Y. X. Wang, J. X. Zhang, X. J. Pu, X. P. Ai, Z. X. Chen, H. X. Yang, Y. L. Cao, *Nano Energy*, 2019, 56, 160
 80. Y. M. Yin, F. Y. Xiong, C. Y. Pei, Y. A. Xu, Q. Y. An, S. S. Tan, Z. C. Zhuang, J. Z. Sheng, Q. D. Li, L. Q. Mai, *Nano Energy*, 2017, 41, 452
 81. M. Zhou, W. Li, T. T. Gu, K. L. Wang, S. C. Cheng, K. Jiang, *Chemical Communications*, 2015, 51, 14354
 82. T. Yuan, J. F. Ruan, W. M. Zhang, Z. P. Tan, J. H. Yang, Z. F. Ma, S. Y. Zheng, *ACS Appl. Mater. Interfaces*, 2016, 8, 35114
 83. J. F. Ruan, T. Yuan, Y. P. Pang, S. N. Luo, C. X. Peng, J. H. Yang, S. Y. Zheng, *Carbon*, 2018, 126, 9
 84. Y. Zhang, Y. S. Huang, G. H. Yang, F. X. Bu, K. Li, I. Shakir, Y. X. Xu, *ACS Appl. Mater. Interfaces*, 2017, 9, 15549
 85. Y. S. Huang, K. Li, J. J. Liu, X. Zhong, X. F. Duan, I. Shakir, Y. X. Xu, *J. Mater. Chem. A*, 2017, 5, 2710
 86. B. Wang, W. Yuan, X. Zhang, M. Xiang, Y. Zhang, H. Liu, H. Wu, *Inorganic Chemistry*, 2019, 58(13), 8841–8853
 87. S. Wang, L. Xia, Le Yu, L. Zhang, H. Wang, X. W. D. Lou, *Adv. Energy Mater.*, 2016, 6, 1502217
 88. Y. W. Wang, N. Xiao, Z. Y. Wang, Y. C. Tang, H. Q. Li, M. L. Yu, C. Liu, Y. Zhou, J. S. Qiu, *Carbon*, 2018, 135, 187
 89. M. L. Sun, Z. Z. Wang, J. F. Ni, L. Li, *Adv. Funct. Mater.*, 2017, 30, 1910043
 90. B. Long, J. N. Zhang, L. Luo, G. F. Ouyang, M. S. Balogun, S. Q. Song, Y. X. Tong, *J. Mater. Chem. A*, 2019, 7, 2626
 91. S. Choi, D. Lee, G. Kim, Y. Y. Lee, B. Kim, J. Moon, W. Shim, *Adv. Funct. Mater.*, 2017, 27, 1702244
 92. K. Zhang, X. Zhang, W. He, W. Xu, G. Xu, X. Yi, X. Yang, J. Zhu, *Journal of Materials Chemistry A*, 2019, 7, 9890
 93. Y. Liu, Y. J. Fang, Z. W. Zhao, C. Z. Yuan, X. W. Lou, *Advanced Energy Materials*, 2019, 9, 1803052
 94. W. Zhang, Y. T. Liu, C. J. Chen, Z. Li, Y. H. Huang, X. L. Hu, *Small*, 2015, 11, 3822
 95. D. Kong, Y. Wang, S. Huang, Y. von Lim, J. Zhang, L. Sun, B. Liu, T. Chen, P. Valdivia y Alvarado, H. Y. Yang, *J. Mater. Chem. A*, 2019, 7, 12751
 96. W. H. Chen, X. X. Zhang, L. W. Mi, C. T. Liu, J. M. Zhang, S. Z. Cui, X. M. Feng, Y. L. Cao, C. Y. Shen, *Adv. Mater.*, 2019, 31, 1806664
 97. D. L. Chao, C. H. Lai, P. Liang, Q. L. Wei, Y. S. Wang, C. R. Zhu, G. Deng, V. V. T. Doan Nguyen, J. Y. Lin, L. Q. Mai, et al, *Adv. Energy Mater.*, 2018, 8, 1800058
 98. D. Sun, X. B. Zhu, B. Luo, Y. Zhang, Y. G. Tang, H. Y. Wang, L. Z. Wang, *Advanced Energy Materials*, 2018, 8, 1801197
 99. C. Lu, Z. Z. Li, L. H. Yu, L. Zhang, Z. Xia, T. Jiang, W. J. Yin, S. X. Dou, Z. F. Liu, J. Y. Sun, *Nano Research*, 2018, 11, 4614
 100. Z. Sun, Y. Liu, D. Wu, K. Tan, L. Hou, C. Yuan, *Nanoscale*, 2020, 12, 4119
 101. D. L. Guo, J. W. Qin, C. Z. Zhang, M. H. Cao, *Crystal Growth & Design*, 2018, 18, 3291
 102. G. Y. Zhou, Y. E. Miao, Z. X. Wei, L. L. Mo, F. L. Lai, Y. Wu, J. M. Ma, T. X. Liu, *Adv. Funct. Mater.*, 2018, 28, 1804629
 103. X. Xu, K. Lin, D. Zhou, Q. Liu, X. Qin, S. Wang, S. He, F. Kang, B. Li, G. Wang, *Chem*, 2020, 6, 902
 104. W. Ling, N. Fu, J. Yue, X.-X. Zeng, Q. Ma, Q. Deng, Y. Xiao, L.-J. Wan, Y.-G. Guo, X.-W. Wu, *Adv. Energy Mater.*, 2020, 10, 1903966
 105. Q. Ni, Y. Bai, Y. Li, L. M. Ling, L. M. Li, G. H. Chen, Z. H. Wang, H. X. Ren, F. Wu, C. Wu, *Small*, 2018, 14, 1702864
 106. W. Wang, Q. Xu, H. Liu, Y. Wang, Y. Xia, *Journal of Materials*

- Chemistry A*, 2017, 5, 8440
107. J. Dong, G. M. Zhang, X. G. Wang, S. Zhang, C. Deng, *Journal of Materials Chemistry A*, 2017, 5, 18725
 108. Y. Wang, D. Z. Kong, S. Z. Huang, Y. M. Shi, M. Ding, Y. V. Lim, T. T. Xu, F. M. Chen, X. J. Li, H. Y. Yang, *J. Mater. Chem. A*, 2018, 6, 10813
 109. B. He, P. Man, Q. Zhang, H. Fu, Z. Zhou, C. Li, Q. Li, L. Wei, Y. Yao, *Nano-Micro Letters*, 2019, 11, 1
 110. F. Tao, L. Qin, Y. Chu, X. Zhou, Q. Pan, *ACS Appl. Mater. Interfaces*, 2019, 11, 3136
 111. Y. H. Zhu, S. Yuan, D. Bao, Y. B. Yin, H. X. Zhong, X. B. Zhang, J. M. Yan, Q. Jiang, *Adv. Mater.*, 2017, 29, 1603719
 112. J.-Z. Guo, Z.-Y. Gu, X.-X. Zhao, M.-Y. Wang, X. Yang, Y. Yang, W.-H. Li, X.-L. Wu, *Adv. Energy Mater.*, 2019, 9, 1902056
 113. D. L. Guo, J. W. Qin, Z. G. Yin, J. M. Bai, Y. K. Sun, M. H. Cao, *Nano Energy*, 2018, 45, 136
 114. S. Chen, C. Wu, L. Shen, C. Zhu, Y. Huang, K. Xi, J. Maier, Y. Yu, *Adv. Mater.*, 2017, 29, 1700431
 115. Y. Yao, Z. Wei, H. Wang, H. Huang, Y. Jiang, X. Wu, X. Yao, Z.-S. Wu, Y. Yu, *Adv. Energy Mater.*, 2020, 10, 1903698
 116. H. Ragones, A. Vinegrad, G. Ardel, M. Goor, Y. Kamir, M. M. Dorfman, A. Gladkikh, D. Golodnitsky, *J Electrochem Soc*, 2019, 167, 070503
 117. D. Xie, M. Zhang, Y. Wu, L. Xiang, Y. Tang, *Adv. Funct. Mater.*, 2020, 30, 1906770
 118. D. G. Mackanic, T.-H. Chang, Z. Huang, Y. Cui, Z. Bao, *Chemical Society Reviews*, 2020, 49, 4466
 119. C. Y. Chan, Z. Wang, H. Jia, P. F. Ng, L. Chow, B. Fei, *Journal of Materials Chemistry A*, 2021, 9, 2043
 120. H. S. Li, Y. Ding, H. Ha, Y. Shi, L. L. Peng, X. G. Zhang, C. J. Ellison, G. H. Yu, *Adv. Mater.*, 2017, 29, 1700898
 121. A. Fakharuddin, H. Li, F. Di Giacomo, T. Zhang, N. Gasparini, A. Y. Elezzabi, A. Mohanty, A. Ramadoss, J. Ling, A. Soultati, et al, *Adv. Energy Mater.*, 2021, 11, 2101443
 122. F. Mo, G. Liang, Z. Huang, H. Li, D. Wang, C. Zhi, *Adv. Mater.*, 2020, 32, 1902151
 123. Z. W. Xi, X. Zhang, Y. S. Ma, C. Zhou, J. Yang, Y. Q. Wu, X. J. Li, Y. F. Luo, D. Y. Chen, *ChemElectrochem*, 2018, 5, 3127
 124. Z. W. Guo, Y. Zhao, Y. X. Ding, X. L. Dong, L. Chen, J. Y. Cao, C. C. Wang, Y. Y. Xia, H. S. Peng, Y. G. Wang, *Chem*, 2017, 3, 348
 125. D. Zhou, L. Xue, L. Wang, N. Wang, W.-M. Lau, X. Cao, *Nano Energy*, 2019, 61, 435
 126. a) E. J. Lee, T. Y. Kim, S.-W. Kim, S. Jeong, Y. Choi, S. Y. Lee, *Energy Environ. Sci.* 2018, 11, 1425; b) C. K. Jeong, K.-I. Park, J. H. Son, G.-T. Hwang, S. H. Lee, D. Y. Park, H. E. Lee, H. K. Lee, M. Byun, K. J. Lee, *Energy Environ. Sci.* 2014, 7, 4035; c) C. Zhang, Y. Fan, H. Li, Y. Li, L. Zhang, S. Cao, S. Kuang, Y. Zhao, A. Chen, G. Zhu et al., *ACS Nano* 2018, 12, 4803
 127. M. Xie, Y. Zhang, M. J. Krasny, C. Bowen, H. Khanbareh, N. Gathercole, *Energy Environ. Sci.*, 2018, 11, 2919
 128. Z. L. Wang, *Adv. Mater.*, 2009, 21, 1311
 129. H. He, Y. Fu, T. Zhao, X. Gao, L. Xing, Y. Zhang, X. Xue, *Nano Energy*, 2017, 39, 590
 130. X. Xue, P. Deng, S. Yuan, Y. Nie, B. He, L. Xing, Y. Zhang, *Energy Environ. Sci.*, 2013, 6, 2615
 131. X. Xue, S. Wang, W. Guo, Y. Zhang, Z. L. Wang, *Nano Lett.*, 2012, 12, 5048
 132. X. Xue, P. Deng, B. He, Y. Nie, L. Xing, Y. Zhang, Z. L. Wang, *Adv. Energy Mater.*, 2014, 4, 1301329

133. A. Ramadoss, B. Saravanakumar, S. W. Lee, Y.-S. Kim, S. J. Kim, Z. L. Wang, *ACS Nano*, 2015, 9, 4337
134. Q. Zheng, B. Shi, Z. Li, Z. L. Wang, *Adv. Sci.*, 2017, 4, 1700029



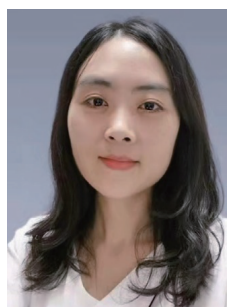
©2022 The Authors. *Materials Lab* is published by Lab Academic Press. This is an open access article under the terms of the Creative Commons Attribution License, which permits use, distribution and reproduction in any medium, provided the original work is properly cited.

Biographies



carbon anode materials for alkali metal batteries.

Xiang-Xi He is received his M.S. degree from School of Environmental and Chemical Engineering, Shanghai University in 2021. Currently he is a doctoral candidate in the School of Environmental and Chemical Engineering, Shanghai University. His research focuses on the structural design, mechanistic investigation and commercialization of advanced



Li Li now works at Shanghai University. She obtained her Ph.D. degree from the University of Wollongong in 2014. Her research interests are mainly focused on the fabrication of materials and their application in rechargeable batteries, including lithium-ion batteries, sodium-ion batteries, and potassium-ion batteries.



applications, especially novel composite materials, new binders, and new electrolytes for Li/Na batteries.

Shu-Lei Chou is a distinguished professor at the Institute of Carbon Neutralization, Wenzhou University. He obtained his Bachelor's degree (1999) and Master's degree (2004) from the Nankai University, China. He received his Ph.D. degree from the University of Wollongong in 2010. His research interests include energy storage materials for battery